W. KOLLER and F. SCHÜRRER (*)

Conservative solution methods
for extended Boltzmann equations (**)

1 - Introduction

1.1 - *General remarks*

In the field of kinetic theory of dilute gases [1], [2] much effort has already been made to tackle the nonlinear Boltzmann equation (BE) which governs the temporal evolution of the phase space distribution density of simple elastically interacting particles. Current research expands upon the original BE in a way that allows different kinds of interactions between various particles to be taken into account. These extensions of the BE to particles in different quantum states as well as to photon interactions and chemical reactions have become increasingly important. The reason for this is that a macroscopic description fails if one has to deal with non-equilibrium states. Fast exothermic gas phase reactions or dissociation and recombination processes in shock waves are typical situations in which the equilibrium particle distribution is highly disturbed, and therefore, the usual concept of evaluating the rate constants does not apply [3].

In general, the BE opposes a rigorous mathematical solution. Consequently, one observes the trend to idealize the BE in order to gain mathematically rigorous solutions - of course without violating fundamental physical laws [4], [5], [6], [7], [8], [9], [10], [11], [12], [13]. This method provides important insight into the approach to equilibrium for initially disturbed systems. Connections between anomalies in the

(*) Institut für Theoretische Physik, Technische Universität Graz, Graz, Austria.

temporal relaxation of the distribution function and the nonlinear structure of the BE also become evident. These investigations have proven to be highly complex even for spatially homogeneous gases with isotropic velocity distributions.

Due to its mathematical complexity, approximation methods for solving the BE have been developed. Attempts in connection with a linearization of the BE have led to various approximate solutions (e.g. the well-known *Chapman-Enskog* perturbation method). However, today much effort is being made to solve the BE in its nonlinear form. Stable and rigorously conserving multigroup procedures [14] were applied to solve the BE for homogeneous isotropic gases and gas mixtures. Interesting effects such as overshooting even at low energies were observed [15]. The range of validity of the heat bath approximation which allows a linearization or the Rayleigh and Lorentz gas approximation were examined [16]. For purely numerical solutions, Monte Carlo Methods [17] and Lattice gas automata [18] are popular. Most activities in the field of analytical solutions focus either on developing nonlinear perturbation methods or on solving equations by using *Lie* groups.

Moreover, the discrete kinetic theory [19], [20], [21], [22], [23], [24] offers an alternative way for treating such problems. The common feature of discrete velocity models is that particles may only receive values of a discrete and usually finite set of velocities in one to three dimensions. Microscopic energy and momentum conservation single out possible binary (or higher order) collisions. The mathematical description of discrete velocity models results in a system of coupled nonlinear partial differential equations, hence reducing the complexity of the mathematical description in comparison to the continuous case, where one has to treat an integro-differential equation. Although this approach seems to be very promising, current research activities exhibit that one is faced with some new difficulties, e.g., a correct temperature definition [25], [26], scaling problems or dealing with external force terms.

1.2 - *Extension to inelastic scattering*

The extended kinetic theory deals with the dynamics of a rarefied gas if effects of non-conservative interactions are considered together with the usual elastic scattering mechanisms. It is the combination of nonlinearity and nonconservativity due to absorptions, creations, chemical and nuclear reactions that gives rise to the most interesting dynamical behaviors (cf. [12]). A successful step in this direction was the generalization of the *Krook-Wu*-model in order to describe these types of interactions [27] by means of scalar BEs. The thermalization of «hot» postcollisional molecules in the «cold» gas led to an overpopulation of the

distribution function at high energies and to remarkable deviations of the transition rates from those obtained by the macroscopic approach [28]. Pioneering considerations in the case of inelastic scattering of particles with internal energy levels have been made by *Garibotti* and *Spiga* [29] who suggest treating unequal quantum states as different species and provide the corresponding Boltzmann-like equations. They study the transport of point particles A which can scatter elastically and inelastically with particles B,

$$(1) \qquad\qquad A + B \rightleftharpoons A + B^*$$

where B^* denotes the excited particle B. For formal simplicity, the authors allow only two discrete internal states separated by a fixed energy step and find exact solutions of the BE for simple test cases related to the transport of electrons and neutrons in gases. Normally, the density of electrons or neutrons propagating in media is much smaller than the density of the medium so that nonlinear terms are not required and the BE becomes linear. An H-theorem is derived and conservation of mass, momentum and total energy is proven.

By substituting in (1) the point particles A with monochromatic photons one is led to the field of radiation gas dynamics [30]. A BE for a system of two-level atoms interacting with monochromatic photons is introduced by *Rossani*, *Spiga* and *Monaco* [31]. Their setup allows for all physically possible inelastic mechanisms of exchange between the two internal energy levels. Rigorous Boltzmann elastic and inelastic collision terms for particle-particle collisions are introduced and a kinetic equation for photons describes the evolution of the radiation field. The approach to equilibrium is proved by establishing a Boltzmann inequality for the system whose radiation distribution is found to approach the well-known Planck function. *Rossani* and *Spiga* [32] have generalized the model and taken into account an arbitrary finite number of internal energy levels. Again transitions between different energy levels may occur by inelastic scattering as well as by absorption or emission of photons of the self-consistent radiation field. The model shows a trend towards equilibrium where a mass action law is valid and radiation intensities are described by Planck's law of radiation. On integrating the Boltzmann equation *Rossani* and *Spiga* derive five fluid dynamical conservation equations corresponding to the conservation of mass, momentum and total (kinetic and internal) energy. A swarm of one level test particles diffusing in a scattering background of N-level field particles is treated with the same methods leading to a linear BE for the test particles. It is interesting to note that, in the Lorentz gas limit, the equilibrium distribution of the test particles is only a Maxwellian if at least one ratio of two internal energy jumps is irrational. This is due to an infinite number of colli-

sion invariants (cf. [**33**], [**34**]), or, in the framework of hydrodynamics, to an infinite number of conservation laws.

In the study of chemical reactions, gas kinetic approaches based on Boltzmann-like equations have a long tradition. The first calculations in this field were made by *Prigogine* and coworkers [**35**], [**36**], who solved the BE for a dilute gas undergoing the reaction $A + A \rightarrow products$. A short summary of the development up to 1990 can be found in [**37**]. Furthermore, the authors considered a spatially homogeneous mixture of rarefied gases of N different species interacting through binary collisions.

By means of a multigroup discretization, *Kügerl* [**38**], [**39**] solved scalar Boltzmann equations for a gas mixture of four species A, B, C, D in which a reversible bimolecular reaction $A + B \rightleftharpoons C + D$ occurs. He found that due to translational non-equilibrium effects, the correction of the chemical rate constants are noticeable depending on the heat of reaction, the activation energy and the steric factor. The result is a shortening of the reaction period by up to 25%. In [**40**], *Rossani* and *Spiga* applied the extended kinetic theory to bimolecular chemical reactions. Conservation of mass, momentum and energy were correctly taken into account. The mass action law in equilibrium is recovered as well as the explicit form of the collision terms discussed. In [**41**], inelastic scattering is described as a particular case of binary reactions when products coincide with reactants; however, one of the products is in an excited state (cf. Eq. (1)). An extension of the formalism to a chemically reacting gas mixture whose particles are additionally endowed with internal energy levels can be found in [**42**].

Based on the formalism used in [**29**], *Rossani* [**43**] applies the linear BE for inelastic scattering to the study of the distribution function for charged particles. These particles propagate in a host medium reacting according to (1) with the field particles. Furthermore, they are subjected to an external electric field. The inelastic collision integral is studied and the equilibrium distribution is investigated. Connections with the transport of electrons in a semiconductor are pointed out. A Fokker-Planck approximation, usually applied in the Physics of Weakly Ionized Gases, is adapted to the situation and leads to a solvable system for the first two moments of the distribution function. The author gives explicit results for the cases of Maxwell and hard sphere interactions. In the framework of extended kinetic theory, *Fontana* and *Spiga* derive a linear one-dimensional BE that models propagation of a swarm of test particles in an absorbing and inelastic down-scattering background [**44**]. As a physical application, the authors use a rigorous algorithm to calculate the penetration of a beam of test particles into a plane slab under steady state conditions. Numerical results are discussed with emphasis on the most significant parameters relevant to radiation shielding. In [**45**], *Banasiak*,

Frosali and *Spiga* reconsider the same model from a more mathematical point of view. Up scattering is again neglected compared to down scattering. This yields to an energy interval in which test particles remain unscattered. In a natural way, the model singles out a Knudsen number ε whose limit $\varepsilon \to 0$ is investigated and leads to hydrodynamic equations of the streaming type. After analyzing the collision mechanism, the hydrodynamic quantity, which is appropriate for the situation of only down scattering, is introduced. The properties of the zero eigenvalue of the collision operator are studied.

The model of a Lorentz gas (light test particles interacting with a given background of heavy field particles at rest), has proved to be very useful for clarifying different properties of solutions of linear and nonlinear kinetic problems (for a historical example see [46]). *Bobylev* and *Spiga* [47] generalize this powerful tool to the linear extended kinetic theory by proposing a Lorentz-type model which allows for absorption and for inelastic scattering between a swarm of test particles and a background of heavy field particles. Attention is focused on the case in which elastic and inelastic scattering are equally important and prevailing with respect to absorption and streaming. Small mean free path asymptotics is studied and an approximate equation at a macroscopic level with first order corrections in the Knudsen number ε is deduced. Like in [32], the null space of the collision operator is found to be infinitely dimensional and an *H*-theorem is established.

In the spirit of neutron transport and nuclear reactor calculations, *Caraffini*, *Ganapol* and *Spiga* [48] propose a multigroup approximation to the nonlinear BE. Their starting point is the scattering kernel formulation of the BE, whose equivalence to the standard formulation of the BE has been proved in [49] and [50]. They consider a single species gas diffusing in a scattering and absorbing background. In this framework, the presence of an external force and an external source can properly be taken into account. The authors compare their approach to the corresponding semi-continuous kinetic models showing quite a different mathematical structure unable to deal with external force terms.

In semi-continuous models, the velocity moduli are discretized while keeping full angular dependence in the velocity space [51], [52]. In [53], *Preziosi* and *Longo* investigate the general discretization problem that is the link between the continuous and discretized BE. They propose a fully controllable model starting from the actual continuous kinetic equations and discretizing the speed variable by a suitable interpolation procedure. The paper clarifies what kind of approximations are involved in the transition from the continuous to the semi-continuous description. The order of magnitude of the spurious terms appearing in the hydrodynamic limit of a discretized BE is investigated as a «distance» between the discreti-

zed model and the full BE. By applying an interpolation approximation like in [53], *Spiga* [54] shows that on account of the microreversibility properties of the scattering kernel, the conservation of mass, momentum and energy as well as an *H*-theorem for the resulting semi-continuous model hold. Thus, the author establishes an intrinsic conservation of momentum and energy conservation and an *H*-theorem for the multigroup approach of [48].

In [55], *Rossani* and *Spiga* present a two-group approximation of the non-linear BE. By improving the approach in [48], the conservation of momentum and energy is intrinsic to the paper's setup independent of the number of groups considered. It is shown that the macroscopic equations can be made self-consistent by a Maxwell-Cattaneo equation for the heat flux. On the basis of assumptions on the scattering kernels only, a correct trend versus time and a physically meaningful definition of the transport coefficients are guaranteed by this very simple model. A P_1-approximation (a tool widely utilized in linear transport theory) is generalized to the nonlinear theory in order to get information on the fluid dynamics of the model.

The 13 moment method, proposed by *Grad* [56], [57] for the solution of the BE, has constituted the basis of a new theory in mathematical physics, namely the so-called extended thermodynamics [58]. *Grad's* procedure represents the distribution function as a truncated Hermite polynomial expansion in which only the moments of interest are retained. This leads to a closed set of moment equations for the BE. In [59], *Cavazzoni* and *Spiga* take the first step towards the employment of the 13 moment approach in the frame of the extended kinetic theory. Confining themselves to elastic scattering of Maxwell molecules, the authors derive the relevant 13 moment equations for a mixture of several participating gases (TP) in the presence of one or more background species (FP). Small mean free path asymptotics show quite different scenarios depending on the relative importance of TP-TP collisions on the one hand and TP-FP collisions on the other.

Dealing with spatial dependent problems in extended kinetic theory requires not only the treatment of the speed variable of the distribution function, but also the direction dependence of the particle velocities. Semi-continuous models are a very efficient way to treat the speed dependence. In order to deal with the direction dependence of the velocities an expansion in terms of spherical harmonics applies. Overlapping multigroup methods are an alternative way to treat the speed dependence. These methods as well as the technique of non-linear spline interpolations have – in contrast to the first method – the advantage that external fields can be dealt with in a natural way.

This paper is organized as follows: After this report of recent approaches to solve extended nonlinear BEs, Sec. **2** provides a set of extended semi-continuous

kinetic equations governing the evolution of a gas mixture. The model takes into account collision excitation and de-excitation processes as well as the interaction with monochromatic photons. Conservation properties and an H-theorem are established.

Section 3 is devoted to the derivation of the P_N multigroup equations for arbitrary scattering models. The truncated moment equations display rigorously conservation of mass and energy, while showing the conservation of momentum requires the numerical treatment of one integral.

In Sec. 4 the methods developed in Sec. 2 and 3 are applied to some test cases like high frequency acoustic waves occurring in degenerate four wave mixing (DFWM) experiments and the propagation of a hot spot within a cold medium.

A semi-continuous model for chemical reactions is the content of Sec. 5. A four species gas mixture undergoing chemical reactions is treated by means of a set of semi-continuous BEs. The model is solved numerically by resorting to a P_0 approximation for spatially homogeneous situations.

The last part of the paper presents multigroup approaches to extended BE. Section 6 sketches the overlapping multigroup approach that allows one to treat external force terms in a natural manner. This is illustrated on a three-dimensional Lorentz gas model. Results are obtained in P_1 approximation. The following Sec. 7 contains the ingredients of a more flexible approach. Instead of working with rigid shape functions as in the overlapping multigroup approach, a spline interpolation of the speed-dependence of the distribution function is proposed. Finally, Sec. 8 generalizes this idea. Expanding the speed dependence of the distribution function in terms of Legendre polynomials within compact speed intervals opens the possibility of a stable and numerically efficient scheme for the solution of the nonlinear BE.

2 - Semi-continuous extended kinetic theory

In a recently published paper [53], *Preziosi* and *Longo* provide a semi-continuous formulation of the nonlinear Boltzmann equation. This formulation is done in terms of a set of distribution functions f_i depending on a solid angle $\widehat{\boldsymbol{\Omega}}$, the spatial position $\boldsymbol{x}$ and time t. In discretizing the kinetic energies (*i.e.* the moduli of the velocity) of the particles (subscript i), the authors reduce the complexity of the integrals in the collision term.

In fact, the collision operator of semi-continuous models contains only integrals over compact domains (parts of the two-dimensional sphere). Physically

speaking, this operator describes the hopping of the gas particles from one energy group i to another i' due to binary collisions. In leaving a continuous set of allowed directions of velocities, semi-continuous models provide a larger and more realistic set of possible outcomes of binary collision processes than discrete velocity models, where only a finite set of different velocities is accounted for [22].

A great advantage of the semi-continuous approach in numerical implementations is that the remaining integrals can be treated, e.g., by resorting to an expansion of the distribution functions in terms of spherical harmonics with respect to the solid angles $\widehat{\boldsymbol{\Omega}}$. This aspect is investigated in [60] and [61] and will be discussed in Sec. 3.

2.1 - *Semi-continuous kinetic equations*

Here, we generalize the ideas of *Preziosi* and *Longo* [53] in order to cope with problems in the field of extended kinetic theory. To this end, we consider a gas mixture composed of three species, namely A, B and B^*, where B^* is an excited state of B. The energy gap between B^* and B is denoted by $\Delta E > 0$. We take into account all elastic scattering processes of the form $N + M \rightleftharpoons N + M$ for N, $M = A$, B, B^* as well as the inelastic interaction (collision excitation and de-excitation)

$$A + B \rightleftharpoons A + B^*. \tag{2}$$

Furthermore, we assume that transitions between B and its excited state B^* can also be induced by monochromatic photons. Therefore, we include the reactions

$$B + p \rightleftharpoons B^*, \qquad B^* + p \rightarrow B + 2p, \tag{3}$$
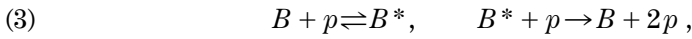
where p denotes a photon with frequency $\nu = \Delta E/h$, (h is Planck's constant). Such a situation is, e.g., typical for laser induced thermal acoustics (LITA) experiments [62], where photons (supplied by a strong coherent laser pulse) excite high frequency acoustic waves.

By assuming equal mass m of the three species, we express the conservation of energy E and momentum $\boldsymbol{R}$ in binary collisions as

$$2E/m = v'^2 + v_*'^2 = v^2 + v_*^2 \mp \varepsilon^2, \tag{4}$$

$$\boldsymbol{R}/m = v' \, \widehat{\boldsymbol{\Omega}}' + v_*' \, \widehat{\boldsymbol{\Omega}}_*' = v\widehat{\boldsymbol{\Omega}} + v_* \, \widehat{\boldsymbol{\Omega}}_*, \tag{5}$$

where, for the purpose of the discretization, we have resorted to a polar decompo-

sition of the velocity variable $\boldsymbol{v} = v\widehat{\boldsymbol{\Omega}}$ with $v = |\boldsymbol{v}|$ and the unit vector $\widehat{\boldsymbol{\Omega}} = \boldsymbol{v}/v$. Primed symbols refer to post-collision quantities. The quantity ε equals zero for elastic collisions and is linked with the energy gap ΔE by

$$(6) \qquad \Delta E = \frac{m}{2}\,\varepsilon^2$$

for inelastic collisions. The minus sign in Eq. (4) refers to an excitation event and the plus sign to a de-excitation process.

   We express the post-collision (primed) velocities by means of the sum of the pre-collision velocities and the unit vector $\widehat{\boldsymbol{n}}'$ pointing in the direction of the relative velocity $\boldsymbol{g}' = \boldsymbol{v}' - \boldsymbol{v}'_*$ after the collision:

$$(7) \qquad \boldsymbol{v}' = \frac{\boldsymbol{R}}{2m} + \frac{g'}{2}\,\widehat{\boldsymbol{n}}'\,, \qquad \boldsymbol{v}'_* = \frac{\boldsymbol{R}}{2m} - \frac{g'}{2}\,\widehat{\boldsymbol{n}}'\,,$$

where the relative speed after the collision is given by $g' = g^{\pm} = \sqrt{g^2 \pm 2\varepsilon^2}$ in the case of inelastic collisions and by $g' = g$ in the case of elastic collision. If the post-collision velocity $\boldsymbol{v}'$ results from an (de-) excitation event, we will denote it by $(\boldsymbol{v}^+)\,\boldsymbol{v}^-$. The functions $f \equiv f^A$, $\check{f} \equiv f^B$ and $\widehat{f} \equiv f^{B*}$ describe the phase density of the particles A, B and $B*$, respectively. According to Ref. [29], the inelastic collision terms read

$$(8a) \qquad \mathfrak{J}[f, \widehat{f}, \check{f}\,] = \int\limits_{\mathbb{R}^3} d\boldsymbol{v}_* \int\limits_{S^2} d\widehat{\boldsymbol{n}}'\, g\,\check{\sigma}(g, \gamma)[f(\boldsymbol{v}^+)\,\check{f}(\boldsymbol{v}^+_*) - f(\boldsymbol{v})\,\widehat{f}(\boldsymbol{v}_*)]$$

$$+ \int\limits_{\mathbb{R}^3} d\boldsymbol{v}_* \int\limits_{S^2} d\widehat{\boldsymbol{n}}'\, g\,\widehat{\sigma}(g, \gamma)[f(\boldsymbol{v}^-)\,\widehat{f}(\boldsymbol{v}^-_*) - f(\boldsymbol{v})\,\check{f}(\boldsymbol{v}_*)],$$

$$(8b) \qquad \check{\mathfrak{J}}[f, \widehat{f}, \check{f}\,] = \int\limits_{\mathbb{R}^3} d\boldsymbol{v}_* \int\limits_{S^2} d\widehat{\boldsymbol{n}}'\, g\,\widehat{\sigma}(g, \gamma)[\widehat{f}(\boldsymbol{v}^-)\,f(\boldsymbol{v}^-_*) - \check{f}(\boldsymbol{v})\,f(\boldsymbol{v}_*)],$$

$$(8c) \qquad \widehat{\mathfrak{J}}[f, \widehat{f}, \check{f}\,] = \int\limits_{\mathbb{R}^3} d\boldsymbol{v}_* \int\limits_{S^2} d\widehat{\boldsymbol{n}}'\, g\,\check{\sigma}(g, \gamma)[\check{f}(\boldsymbol{v}^+)\,f(\boldsymbol{v}^+_*) - \widehat{f}(\boldsymbol{v})\,f(\boldsymbol{v}_*)],$$

where $\Theta(.)$ denotes the unit step function and $\cos\gamma = \widehat{\boldsymbol{n}}\cdot\widehat{\boldsymbol{n}}'$. The microreversibility condition [29] linking the up $(\widehat{\sigma})$ and down $(\check{\sigma})$ scattering cross section is given by

$$(9) \quad g^2\widehat{\sigma}(g, \gamma) = \Theta(g - \sqrt{2}\varepsilon)(g^-)^2\check{\sigma}(g^-, \gamma) \quad \text{and} \quad g^2\check{\sigma}(g, \gamma) = (g^+)^2\widehat{\sigma}(g^+, \gamma).$$

The collision terms describing the impact of elastic scattering between particles N and M on the evolution of N are of the form

$$(10) \qquad J^{NM} = \int\limits_{\mathbb{R}^3} d\boldsymbol{v}_* \int\limits_{\mathbb{S}^2} d\widehat{\boldsymbol{n}}' \, g\sigma(g, \gamma)[f^N(\boldsymbol{v}') \, f^M(\boldsymbol{v}'_*) - f^N(\boldsymbol{v}) \, f^M(\boldsymbol{v}_*)],$$

with the elastic cross section σ. These terms constitute the right hand side of the continuous Boltzmann equations of the model:

$$(11a) \qquad \frac{\partial f}{\partial t} + v\widehat{\boldsymbol{\Omega}} \cdot \frac{\partial f}{\partial \boldsymbol{x}} = \mathfrak{J} + J^{AA} + J^{AB} + J^{AB^*},$$

$$(11b) \qquad \frac{\partial \check{f}}{\partial t} + v\widehat{\boldsymbol{\Omega}} \cdot \frac{\partial \check{f}}{\partial \boldsymbol{x}} = \check{\mathfrak{J}} - \mathcal{R}(I) + J^{BB} + J^{BA} + J^{BB^*},$$

$$(11c) \qquad \frac{\partial \widehat{f}}{\partial t} + v\widehat{\boldsymbol{\Omega}} \cdot \frac{\partial \widehat{f}}{\partial \boldsymbol{x}} = \widehat{\mathfrak{J}} + \mathcal{R}(I) + J^{B^*B^*} + J^{B^*A} + J^{B^*B}.$$

The interaction with monochromatic photons of intensity I is modeled by means of Einstein coefficients α (for spontaneous emission) and β (for absorption and stimulated emission). Neglecting the Doppler effect, the photon-particle interaction term reads

$$(12) \qquad \mathcal{R}(I) = \int\limits_{\mathbb{S}^2} d\widehat{\boldsymbol{\Omega}}_* (\beta I(\widehat{\boldsymbol{\Omega}}_*) \, \check{f}(\boldsymbol{v}) - (\alpha + \beta I(\widehat{\boldsymbol{\Omega}}_*)) \, \widehat{f}(\boldsymbol{v})),$$

where I denotes the specific intensity of photons with energy ΔE. The evolution equation for the specific intensity $I(t, \boldsymbol{x}, \widehat{\boldsymbol{\Omega}})$ is given by [63]

$$(13) \qquad \frac{\partial I}{\partial t} + c\widehat{\boldsymbol{\Omega}} \cdot \frac{\partial I}{\partial \boldsymbol{x}} = \frac{\partial I_L}{\partial t} - c\Delta E \int\limits_{\mathbb{R}^3} d\boldsymbol{v} \, (\beta I \check{f}(\boldsymbol{v}) - (\alpha + \beta I) \, \widehat{f}(\boldsymbol{v})),$$

where c stands for the speed of light and $I_L(t, \boldsymbol{x}, \widehat{\boldsymbol{\Omega}})$ is an impressed time dependent intensity profile of light. The energy density e_ν, the energy flux $\boldsymbol{Q}_\nu$ and the energy density $\mathcal{S}_L$ of the impressed light are respectively defined by

$$(14) \qquad e_\nu = \frac{1}{c} \int\limits_{\mathbb{S}^2} I(\widehat{\boldsymbol{\Omega}}) \, d\widehat{\boldsymbol{\Omega}}, \qquad \boldsymbol{Q}_\nu = \int\limits_{\mathbb{S}^2} \widehat{\boldsymbol{\Omega}} I(\widehat{\boldsymbol{\Omega}}) \, d\widehat{\boldsymbol{\Omega}}, \qquad \mathcal{S}_L = \frac{1}{c} \int\limits_{\mathbb{S}^2} I_L(\widehat{\boldsymbol{\Omega}}) \, d\widehat{\boldsymbol{\Omega}}.$$

The conservation of mass, momentum and energy as well as an H-theorem for the inelastic collision terms of the above sketched model are provided in Ref. [29].

A derivation of Planck's law of radiation (for $I_L = 0$) and an H-function for the photon transport equation can be found in Ref. [**31**].

In order to discretize the kinetic equations describing the evolution of the gas mixture and the photon intensity constituted by Eqs. (11) and (13), we apply a generalized form of the procedure introduced in [**53**]. Following these lines, we restrict the range of the particle's kinetic energies to the interval $I_\nu = [E_m, E_M)$, $0 < E_m < E_M < \infty$. The bounds of I_ν are to be chosen such that all particles with kinetic energies outside of I_ν may be neglected. Next we introduce an arithmetic sequence of energies

$$(15) \qquad E_i = E_m + \left(i + \frac{1}{2} \right) \delta , \qquad i = 0, 1, \ldots, n ,$$

with $\delta = (E_M - E_m)/(n + 1)$ that are the centers of the subintervals (energy groups)

$$(16) \qquad I_i = \left[E_i - \frac{\delta}{2} , E_i + \frac{\delta}{2} \right], \qquad i = 0, 1, \ldots, n .$$

Furthermore, we have to adapt the energy gap ΔE in such a way that it fits into the discretization scheme. Therefore, we set $\Delta E = q\delta$ with $q \in \{1, 2, \ldots, 2n - 1\}$ which implies $\varepsilon^2 = 2q\delta/m$. When appearing as an integrand, any function of kinetic energy (and thus of the speed v) is approximated by a piecewise constant interpolant defined over the above stated discretization:

$$(17) \qquad g(E) \approx \sum_{i=0}^{n} g_i \chi_{I_i}(E),$$

where $\chi_B(.)$ denotes the characteristic function of the set B.

Each energy knot E_i corresponds to a speed $v_i = \sqrt{2E_i/m}$. The combination of conservation of momentum and total energy, i.e. Eqs. (4) and (5), implies a restriction on $\widehat{\boldsymbol{\Omega}}_*$ [**64**]. In fact, when fixing $\widehat{\boldsymbol{\Omega}}$, the variation of the solid angle $\widehat{\boldsymbol{\Omega}}_*$ is restricted to

$$(18) \qquad \binom{\widehat{D}_*}{\check{D}_*} = \left\{ \widehat{\boldsymbol{\Omega}}_* \in \mathbb{S}^2 \; \middle| \; - \frac{v' v'_*}{v v_*} \mp \frac{\varepsilon^2}{2 v v_*} \leqslant \widehat{\boldsymbol{\Omega}} \cdot \widehat{\boldsymbol{\Omega}}_* \leqslant \frac{v' v'_*}{v v_*} \mp \frac{\varepsilon^2}{2 v v_*} \right\}.$$

Figure 1 shows a graphical representation of these sets.

For elastic collisions ($\varepsilon = 0$), the inner product $\widehat{\boldsymbol{\Omega}} \cdot \widehat{\boldsymbol{\Omega}}_*$ is symmetric with respect to zero. In this case we define $D_* = \widehat{D}_* = \check{D}_*$. For inelastic excitation ($\widehat{D}_*$) and de-excitation ($\check{D}_*$) processes this is no longer true.
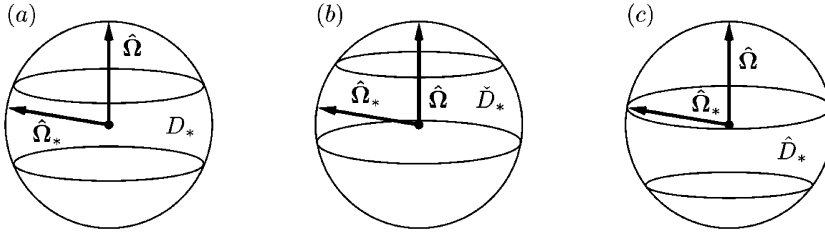
Fig. 1 - Domains of $\widehat{\boldsymbol{\Omega}}_*$ as implied by the conservation of momentum for elastic scattering (a), collision de-excitation (b), and collision excitation (c).

Furthermore, by introducing the angle ϑ between the pre-collision and post-collision plane spanned by the pairs $(\boldsymbol{g}, \boldsymbol{R})$ and $(\boldsymbol{g}', \boldsymbol{R})$, respectively, the surface element $d\widehat{\boldsymbol{n}}'$ appearing in the collision terms can be written as

$$(19) \qquad\qquad d\widehat{\boldsymbol{n}}' = \frac{4}{g'R}\, v'\, dv'\, d\vartheta\,.$$

By following the considerations of Sec. **4** in [**53**], we obtain semi-continuous versions of the inelastic collision terms. We integrate Eqs. (8) over one energy interval I_i with the appropriate measure $\sqrt{2E/m^3}dE = v^2\,dv$ and approximate all functions of kinetic energy by piecewise constant interpolants. If the cross section is independent of the scattering angle, which we shall assume for simplicity, they read

$$(20a) \qquad \mathfrak{J}_i[f,\check{f},\widehat{f}] = C_\chi^2 \sum_{j=0}^{n} v_j \sum_{\substack{h,k=0 \\ h+k=i+j+q}}^{n} \int_0^{2\pi} d\vartheta \int_{\check{D}_*(v_i,v_j,v_h)} d\widehat{\boldsymbol{\Omega}}_*\, \check{A}_{ij}^{hk}(\widehat{\boldsymbol{\Omega}}\cdot\widehat{\boldsymbol{\Omega}}_*)(f_h'\,\check{f}_{*k}' - f_i \widehat{f}_{*j})$$

$$+ C_\chi^2 \sum_{j=0}^{n} v_j \sum_{\substack{h,k=0 \\ h+k=i+j-q}}^{n} \int_0^{2\pi} d\vartheta \int_{\widehat{D}_*(v_i,v_j,v_h)} d\widehat{\boldsymbol{\Omega}}_*\, \widehat{A}_{ij}^{hk}(\widehat{\boldsymbol{\Omega}}\cdot\widehat{\boldsymbol{\Omega}}_*)(f_h'\,\widehat{f}_{*k}' - f_i \check{f}_{*j}),$$

$$(20b) \qquad \check{\mathfrak{J}}_i[f,\check{f},\widehat{f}] = C_\chi^2 \sum_{j=0}^{n} v_j \sum_{\substack{h,k=0 \\ h+k=i+j-q}}^{n} \int_0^{2\pi} d\vartheta \int_{\widehat{D}_*(v_i,v_j,v_h)} d\widehat{\boldsymbol{\Omega}}_*\, \widehat{A}_{ij}^{hk}(\widehat{\boldsymbol{\Omega}}\cdot\widehat{\boldsymbol{\Omega}}_*)(\widehat{f}_h' f_{*k}' - \check{f}_i f_{*j}),$$

$$(20c) \qquad \widehat{\mathfrak{J}}_i[f,\check{f},\widehat{f}] = C_\chi^2 \sum_{j=0}^{n} v_j \sum_{\substack{h,k=0 \\ h+k=i+j+q}}^{n} \int_0^{2\pi} d\vartheta \int_{\check{D}_*(v_i,v_j,v_h)} d\widehat{\boldsymbol{\Omega}}_*\, \check{A}_{ij}^{hk}(\widehat{\boldsymbol{\Omega}}\cdot\widehat{\boldsymbol{\Omega}}_*)(\check{f}_h' f_{*k}' - \widehat{f}_i f_{*j}),$$

where $C_\chi = \delta/m$. The application of the same strategy to the elastic collision terms, i.e. Eq. (10), yields

$$(21) \quad J_i^{NM}[f^N, f^M] = C_\chi^2 \sum_{j=0}^{n} v_j \sum_{\substack{h,k=0 \\ h+k=i+j}}^{n} \int_0^{2\pi} d\vartheta \int_{D_*(v_i, v_j, v_h)} d\widehat{\boldsymbol{\Omega}}_* A_{ij}^{hk}(\widehat{\boldsymbol{\Omega}} \cdot \widehat{\boldsymbol{\Omega}}_*)(f_h^{N'} f_{*k}^{M'} - f_i^N f_{*j}^M),$$

for $N, M = A, B, B^*$. The domain $\widehat{D}_*(v_i, v_j, v_h)$ already takes into account the unit step function $\Theta(g - \sqrt{2}\varepsilon)$. We have used the shorthand notations

$$(22) \qquad f_i^N = f_i^N(\widehat{\boldsymbol{\Omega}}) = f^N(v_i \widehat{\boldsymbol{\Omega}}), \qquad f_{*j}^N = f_j^N(\widehat{\boldsymbol{\Omega}}_*) = f^N(v_j \widehat{\boldsymbol{\Omega}}_*),$$

$$(23) \qquad f_h^{N'} = f_h^N(\widehat{\boldsymbol{\Omega}}') = f^N(v_h \widehat{\boldsymbol{\Omega}}'), \qquad f_{*k}^{N'} = f_k^N(\widehat{\boldsymbol{\Omega}}_*') = f^N(v_k \widehat{\boldsymbol{\Omega}}_*'),$$

where $N = A, B, B^*$. Post-collision solid angles are functions of pre-collision solid angles, of the speeds v_i, v_j, and v_h and of the angle ϑ. The kernels are given by

$$(24) \quad A_{ij}^{hk}(\widehat{\boldsymbol{\Omega}} \cdot \widehat{\boldsymbol{\Omega}}_*) = \frac{4\sigma(g)}{R}, \quad \widehat{A}_{ij}^{hk}(\widehat{\boldsymbol{\Omega}} \cdot \widehat{\boldsymbol{\Omega}}_*) = \frac{4g}{g^-} \frac{\widehat{\sigma}(g)}{R}, \quad \check{A}_{ij}^{hk}(\widehat{\boldsymbol{\Omega}} \cdot \widehat{\boldsymbol{\Omega}}_*) = \frac{4g}{g^+} \frac{\check{\sigma}(g)}{R}.$$

In these formulae, the quantities g, $g^\pm$ and R have to be evaluated at the speed knots,

$$(25) \qquad g = \sqrt{v_i^2 + v_j^2 - 2v_i v_j \widehat{\boldsymbol{\Omega} \cdot \boldsymbol{\Omega}}_*}, \qquad R = \sqrt{v_i^2 + v_j^2 + 2v_i v_j \widehat{\boldsymbol{\Omega} \cdot \boldsymbol{\Omega}}_*}$$

and so on for g^+ and g^-. By applying the same strategy to the streaming part of the Boltzmann equations and equating the result to the above stated collision terms, we obtain the semi-continuous kinetic equations

$$(26a) \qquad \frac{\partial f_i}{\partial t} + v_i \widehat{\boldsymbol{\Omega}} \frac{\partial f_i}{\partial \boldsymbol{x}} = \mathfrak{J}_i + J_i^{AA} + J_i^{AB} + J_i^{AB^*},$$

$$(26b) \qquad \frac{\partial \check{f}_i}{\partial t} + v_i \widehat{\boldsymbol{\Omega}} \frac{\partial \check{f}_i}{\partial \boldsymbol{x}} = \check{\mathfrak{J}}_i - \mathcal{R}_i(I) + J_i^{BB} + J_i^{BA} + J_i^{BB^*},$$

$$(26c) \qquad \frac{\partial \widehat{f}_i}{\partial t} + v_i \widehat{\boldsymbol{\Omega}} \frac{\partial \widehat{f}_i}{\partial \boldsymbol{x}} = \widehat{\mathfrak{J}}_i + \mathcal{R}_i(I) + J_i^{B^*B^*} + J_i^{B^*A} + J_i^{B^*B},$$

with $\mathcal{R}_i(I)$ being defined as Eq. (12) evaluated at the speed knot i, i.e. for $\check{f}_i(\widehat{\boldsymbol{\Omega}})$

and $\widehat{f}_i(\widehat{\boldsymbol{\Omega}})$. The photon transport equation now reads

$$(27) \qquad \frac{\partial I}{\partial t} + c\widehat{\boldsymbol{\Omega}} \cdot \frac{\partial I}{\partial \boldsymbol{x}} = \frac{\partial I_L}{\partial t} - c\varDelta E(\beta I \check{n} - (\alpha + \beta I)\,\widehat{n})).$$

In the semi-continuous formulation, the macroscopic quantities of each species N, namely particle density, the mean velocity, the momentum flux and the kinetic energy flux are respectively given by

$$(28a) \qquad n^N = C_\chi \sum_{i=0}^{n} v_i \int_{\mathbb{S}^2} f_i^N(\widehat{\boldsymbol{\Omega}})\, d\widehat{\boldsymbol{\Omega}}\,,$$

$$(28b) \qquad \boldsymbol{u}^N = \frac{C_\chi}{n^N} \sum_{i=0}^{n} v_i^2 \int_{\mathbb{S}^2} \widehat{\boldsymbol{\Omega}} f_i^N(\widehat{\boldsymbol{\Omega}})\, d\widehat{\boldsymbol{\Omega}}\,,$$

$$(28c) \qquad \mathbb{K}^N = C_\chi m \sum_{i=0}^{n} v_i^3 \int_{\mathbb{S}^2} \widehat{\boldsymbol{\Omega}} \otimes \widehat{\boldsymbol{\Omega}} f_i^N(\widehat{\boldsymbol{\Omega}})\, d\widehat{\boldsymbol{\Omega}}\,,$$

$$(28d) \qquad Q^N = \frac{C_\chi m}{2} \sum_{i=0}^{n} v_i^4 \int_{\mathbb{S}^2} \widehat{\boldsymbol{\Omega}} f_i^N(\widehat{\boldsymbol{\Omega}})\, d\widehat{\boldsymbol{\Omega}}\,.$$

The kinetic energy density of species N is given by the trace $k^N = (1/2)\,\mathrm{tr}\,\mathbb{K}^N$. The total energy density e of the gas is the sum of the kinetic energy densities plus the internal energy density of B^*:

$$(29) \qquad e = k^A + k^B + k^{B^*} + n^{B^*} \varDelta E\,.$$

By using these definitions, we can integrate Eqs. (26) and (27) to obtain the macroscopic equations for the semi-continuous model:

$$(30a) \qquad \frac{\partial n}{\partial t} + \frac{\partial}{\partial \boldsymbol{x}} \cdot (n\boldsymbol{u}) = 0\,,$$

$$(30b) \qquad \frac{\partial}{\partial t}(\check{n} + \widehat{n}) + \frac{\partial}{\partial \boldsymbol{x}} \cdot (\check{n}\check{\boldsymbol{u}} + \widehat{n}\widehat{\boldsymbol{u}}) = 0\,,$$

$$(30c) \qquad m\frac{\partial}{\partial t}(\check{n}\check{\boldsymbol{u}} + \widehat{n}\widehat{\boldsymbol{u}} + n\boldsymbol{u}) + \frac{\partial}{\partial \boldsymbol{x}} \cdot (\mathbb{K} + \check{\mathbb{K}} + \widehat{\mathbb{K}}) = 0\,,$$

$$(30d) \qquad \frac{\partial}{\partial t}(e + e_\nu) + \frac{\partial}{\partial \boldsymbol{x}} \cdot (\boldsymbol{Q} + \check{\boldsymbol{Q}} + \widehat{\boldsymbol{Q}} + \boldsymbol{Q}_\nu + \varDelta E\ n^{B^*} \boldsymbol{u}^{B^*}) = \frac{\partial S_L}{\partial t}\,.$$

They reflect the conservation of particles A, B plus B^*, the conservation of total momentum and injection of energy due to external light sources. Proof of these macroscopic equations involves important properties of the collision terms and is presented in [64].

In order to state the properties of the semi-continuous collision terms for a set of arbitrary functions $\varphi_i^N(\widehat{\boldsymbol{\Omega}})$, $N = A, B, B^*$, we introduce the notation

$$\langle \varphi^N, f^N \rangle = C_\chi \sum_{i=0}^{n} v_i \int_{\mathbb{S}^2} d\widehat{\boldsymbol{\Omega}} \varphi_i^N(\widehat{\boldsymbol{\Omega}}) \, f_i^N(\widehat{\boldsymbol{\Omega}}) .$$

Now we can summarize the main properties of the model: First, the expression

(31)
$$\begin{aligned}
\langle\!\langle \boldsymbol{\varphi}, \boldsymbol{J} \rangle\!\rangle &\equiv \langle \varphi, \mathfrak{J} + J^{AA} + J^{AB} + J^{AB^*} \rangle \\
&+ \langle \check{\varphi}, \check{\mathfrak{J}} + J^{BB} + J^{BA} + J^{BB^*} \rangle + \langle \widehat{\varphi}, \widehat{\mathfrak{J}} + J^{B^*B^*} + J^{B^*A} + J^{B^*B} \rangle
\end{aligned}$$

vanishes for the choices $\varphi_i = 1$, $\check{\varphi}_i = \widehat{\varphi}_i = 0$; $\varphi_i = 0$, $\check{\varphi}_i = \widehat{\varphi}_i = 1$; $\varphi_i = \check{\varphi}_i = \widehat{\varphi}_i = v_i\widehat{\boldsymbol{\Omega}}$ and $\varphi_i = \check{\varphi}_i = v_i^2$, $\widehat{\varphi}_i = v_i^2 + \varepsilon^2$. They correspond to the conservation and balance equations stated in Eqs. (30). Furthermore, we obtain a space homogeneous H-theorem by setting $\varphi_i^N = \log f_i^N$. It reads

(32)
$$\frac{\partial H}{\partial t} \equiv \langle\!\langle \log f, \boldsymbol{J} \rangle\!\rangle \leq 0 .$$

This H-function is zero (collision equilibrium of the gas mixture) if and only if

(33)
$$f_i^N(\widehat{\boldsymbol{\Omega}}) = A^N \exp(v_i \boldsymbol{b} \cdot \widehat{\boldsymbol{\Omega}} - c v_i^2) ,$$

with the constants A^N, $\boldsymbol{b}$, and $c = m/(2 k_B T)$, where T is the temperature and k_B denotes Boltzmann's constant. The ratio between the densities of B^* and B reads

(34)
$$\frac{\widehat{n}}{\check{n}} = \exp\left(-\frac{\Delta E}{k_B T}\right),$$

which is exactly Boltzmann's formula. Finally, in the absence of external light

sources, the equilibrium intensity is given by Planck's law [31]

$$(35) \qquad I = \frac{\alpha/\beta}{\exp\left(\Delta E/(k_B T)\right) - 1} \; .$$

2.2 - *Comparison with exact solutions*

In [**53**], *Preziosi* and *Longo* investigate the fluid dynamic behavior of the semi-continuous model. By working with local Maxwellians, the authors give estimates of the errors in the fluid dynamics that are introduced by the discretization procedure. However, little is said about the quality of the relaxation behavior of the model. Therefore, we show here to what extent the local relaxation described with the full continuous Boltzmann equation coincides with that of the semi-continuous model.

For the nonlinear Boltzmann equation of gas dynamics, analytical solutions exist only in very special cases and for particular interaction models. One exact solution is known for Maxwell molecules whose cross section is inversely proportional to the relative speed. This is the so-called BKW mode [**6**]. Thus it is possible to test the accuracy of the semi-continuous model by performing a comparison with this solution.

Since this analytic solution assumes spatially homogeneous and isotropic conditions, we use the ansatz

$$(36) \qquad f_i(\widehat{\boldsymbol{\Omega}}) = \frac{1}{4\pi v_i} n_i.$$

Apart from the multiplicative constant C_χ, the quantities

$$(37) \qquad n_i = v_i \int_{\mathbb{S}^2} f_i(\widehat{\boldsymbol{\Omega}}) \, d\widehat{\boldsymbol{\Omega}}$$

represent the number of gas particles within the energy group I_i. The evolution equations for the quantities n_i are obtained by integrating Eq. (26a) (simplified to one only elastically interacting species) with respect to $\widehat{\boldsymbol{\Omega}}$:

$$(38) \qquad \frac{dn_i}{dt} = \frac{C_\chi^2}{2} \sum_{j=0}^{n} \sum_{\substack{h,\,k=0 \\ h+k=i+j}}^{n} (I_{hk}^{ij} n_h n_k - I_{ij}^{hk} n_i n_j) \, ,$$

with the integrated cross sections

$$
(39) \qquad I_{ij}^{hk} = \frac{2\pi\kappa}{v_i v_j}
\begin{cases}
\arctan\left(\dfrac{2v_h v_k}{|v_h^2 - v_k^2|} \right) & \text{for } v_h v_k \leq v_i v_j \\[2ex]
\arctan\left(\dfrac{2v_i v_j}{|v_i^2 - v_j^2|} \right) & \text{for } v_h v_k > v_i v_j
\end{cases}
$$

for Maxwell molecules, where the positive parameter κ controls the strength of the interaction.

In three dimensions, the BKW mode [6] for Maxwell molecules is given by

$$
(40) \quad f(x, t) = \frac{2\sqrt{x}}{\sqrt{\pi}(1+\gamma_1)^{3/2}} \exp\left(-\frac{x}{1+\gamma_1} \right) \left\{ 1 + \frac{\gamma_1}{1+\gamma_1} \left(\frac{3}{2} - \frac{x}{1+\gamma_1} \right) \right\},
$$

where x stands for the kinetic energy, $x = v^2/2$, and the temporal evolution of γ_1 is given by

$$
(41) \qquad \gamma_1(t) = \eta e^{-\lambda_2 t}, \qquad -0.4 \leq \eta < 0 .
$$

The quantity λ_2 is a nonlinear eigenvalue of the collision operator. Its value is linked with the strength of the interaction measured by κ. For isotropic scattering, λ_2 is given by

$$
(42) \qquad \lambda_2 = \frac{2}{3}\pi\frac{\kappa}{4} .
$$

For the solution of the semi-continuous model, the kinetic energy is resolved using 175 energy groups. The strength of interaction is taken to be $\kappa = 100$ and the initial data correspond to $\eta = -0.4$.

Figure 2 shows the relaxation for different kinetic energies x in the case of Maxwell molecules. For very low and very high energies ($x \leq 1$ or $x > 4$), the particle density increases whereas for average energies ($1 < x < 4$) it decreases during the evolution. For high energies, the relaxation becomes slower and slower. This behavior is partially due to the decreasing cross section. It is remarkable that not the slightest difference between the BKW mode and the relaxation of the semi-continuous model can be observed. The curves for both cases match.

Another way of showing the precision of the semi-continuous model is the investigation of the nonlinear eigenvalue λ_2. For a given kinetic energy x, this is the only parameter in the BKW mode. Thus, for some energies x, we take the curves of Fig. 2 and adapt the parameter λ_2 of the BKW mode by a least-squares fit.
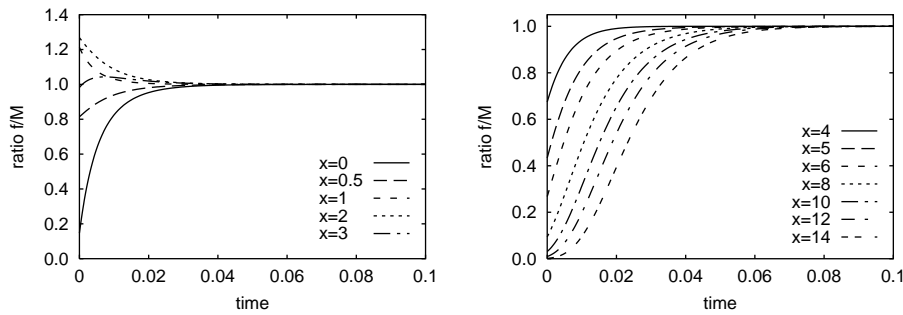
Fig. 2 - Relaxation behavior of Maxwell molecules at different kinetic energies. The curves calculated with the semi-continuous model coincide with those of the analytical solution. The initial distribution in these illustrations coincides with the starting point of the BKW mode at $\eta = -0.4$.

It is very satisfying that they coincide with the exact value within less than 0.2% for average particle speeds. We observe that the discrepancy increases for high speeds. One reason for this behavior is the unphysical but necessary cut-off at v_M. Particles propagating with kinetic energies near the maximum ε_M have a very limited possibility of scattering, because no particles with energies greater than ε_M may result from the collision processes. Nevertheless, even here the discrepancy is less than 1%.

3 - P_N approximation

In non-homogeneous regimes the distribution function depends not only on the modulus of the velocity but also on its direction. In order to treat the direction dependence, moment methods are very convenient.

The P_N method, e.g., has been used very efficiently in the neutron transport theory [65], where a linear form of the Boltzmann equation applies. In the nonlinear case, Jaffé [66] was the first to apply this particular method in the kinetic theory. He confined himself to terms up to second order to obtain solutions of the Boltzmann equation for the case of small Knudsen numbers. In more recent papers, the spherical harmonics method has been generalized to arbitrary order, where the collision term has been included in the expansion scheme [67], [68], [69]. An extension of this method by performing the expansion of the distribution function for a moving reference system in velocity space can be found in [70]. Numerical simulations of thermal and spatial relaxation behavior of a gas of Maxwell molecules in P_1 approximation are given in [60].

Here we discuss the P_N method to the extended semi-continuous Boltzmann equation. We confine ourselves to the one-dimensional case in real space. This means that we expand the distribution functions for each discretized speed in terms of Legendre polynomials with respect to the angle between the velocity and the direction vector in real space. Inserting this ansatz into the semi-continuous Boltzmann equation and projecting it over the Legendre polynomials up to a certain order N results in a closed, coupled set of nonlinear partial differential equations for the moments of the expansion. Since the discretization of the modulus of the particle velocity is performed in such a way that the resulting kinetic energy classes form an arithmetic series [53], we call our method the P_N multigroup approximation.

For simplicity, we demonstrate the method only for the case of elastic scattering (the strategy can easily be extended to inelastic interactions), where the Boltzmann equation for the unknowns $f_i(\widehat{\boldsymbol{\Omega}}, \boldsymbol{x}, t) \overset{\text{def}}{=} f(v_i \widehat{\boldsymbol{\Omega}}, \boldsymbol{x}, t)$ read

$$
\begin{aligned}
& \frac{\partial f_i}{\partial t} + v_i \widehat{\boldsymbol{\Omega}} \cdot \nabla f_i \\
(43) \qquad & = C_\chi^2 \sum_{j=0}^{n} \sum_{\substack{h,k \leq n \\ h+k=i+j}} v_j \int_0^{2\pi} d\vartheta \int_{D_{\widehat{\boldsymbol{\Omega}}_*}(v_i, v_j, v_h)} d\widehat{\boldsymbol{\Omega}}_* A_{ij}^{hk}(\widehat{\boldsymbol{\Omega}} \cdot \widehat{\boldsymbol{\Omega}}_*, \vartheta)(f_h' f_{*k}' - f_i f_{*j}),
\end{aligned}
$$

with the constant $C_\chi = \delta/2$ [53]. Conservation of momentum restricts the domain of integration of the solid angle $\widehat{\boldsymbol{\Omega}}_*$ to the set

$$
(44) \qquad D_{\widehat{\boldsymbol{\Omega}}_*}(v_i, v_j, v_h) = \left\{ \widehat{\boldsymbol{\Omega}}_* : |\widehat{\boldsymbol{\Omega}} \cdot \widehat{\boldsymbol{\Omega}}_*| \leq \frac{v_h v_k}{v_i v_j} \right\}.
$$

The quantities A of Eq. (43) are related to the collision cross section σ and the total momentum of the two colliding particles by

$$
(45) \qquad A_{ij}^{hk}(\widehat{\boldsymbol{\Omega}} \cdot \widehat{\boldsymbol{\Omega}}_*, \vartheta) = 4 \frac{\sigma_{ij}^{hk}(\widehat{\boldsymbol{\Omega}} \cdot \widehat{\boldsymbol{\Omega}}_*, \vartheta)}{R_{ij}(\widehat{\boldsymbol{\Omega}} \cdot \widehat{\boldsymbol{\Omega}}_*)} .
$$

The symbol R denotes the modulus of the total momentum, and the angle ϑ is linked with the angle of deflection. The dependence of the cross section on the relative speed g of the colliding particles is hidden by our notation. The quantities R

and g are defined as

$$(46) \quad R_{ij}(\widehat{\boldsymbol{\Omega}} \cdot \widehat{\boldsymbol{\Omega}}_*) \overset{\text{def}}{=} \sqrt{v_i^2 + v_j^2 + 2v_i v_j \widehat{\boldsymbol{\Omega}} \cdot \widehat{\boldsymbol{\Omega}}_*}, \quad g_{ij}(\widehat{\boldsymbol{\Omega}} \cdot \widehat{\boldsymbol{\Omega}}_*) \overset{\text{def}}{=} \sqrt{v_i^2 + v_j^2 - 2v_i v_j \widehat{\boldsymbol{\Omega}} \cdot \widehat{\boldsymbol{\Omega}}_*},$$

and are preserved under collisions.

We expand the distribution function for each speed in a truncated series of Legendre polynomials P_l. Thus, we assume azimuthal symmetry and account for the N first Legendre moments and make the following ansatz:

$$(47) \quad f_i(\widehat{\boldsymbol{\Omega}}, \boldsymbol{x}, t) = f_i(\cos\theta, z, t) = \sum_{l=0}^{N} a_l^{(i)}(z, t) P_l(\cos\theta).$$

In order to evaluate the streaming term of Eq. (43), we insert the ansatz, Eq. (47), in the LHS of the Boltzmann equation (43), multiply the result by $P_\lambda(\cos\theta)$ and integrate over the angle θ using the measure $\sin\theta d\theta$:

$$(48) \quad \int_0^\pi \sin\theta \, d\theta \, P_\lambda(\cos\theta) \left(\frac{\partial}{\partial t} \sum_{l=0}^{N} a_l^{(i)} P_l(\cos\theta) + v_i \frac{\partial}{\partial x} \cos(\theta) \sum_{l=0}^{N} a_l^{(i)} P_l(\cos\theta) \right).$$

In the case $N = 3$, i.e., when we neglect all Legendre moments higher than 3, we are led to the following set of equations for $\lambda = 0, 1, 2, 3$:

$$(49) \quad \frac{\partial}{\partial t} 2 a_0^{(i)} + v_i \frac{\partial}{\partial x} \frac{1}{3} 2 a_1^{(i)} = \mathfrak{J}_0^{(i)}(\underline{a_0}, \underline{a_1}, \underline{a_2}, \underline{a_3}),$$

$$(50) \quad \frac{\partial}{\partial t} \frac{2}{3} a_1^{(i)} + v_i \frac{\partial}{\partial x} \frac{2}{3} \left(a_0^{(i)} + \frac{2}{5} a_2^{(i)} \right) = \mathfrak{J}_1^{(i)}(\underline{a_0}, \underline{a_1}, \underline{a_2}, \underline{a_3}),$$

$$(51) \quad \frac{\partial}{\partial t} \frac{2}{5} a_2^{(i)} + v_i \frac{\partial}{\partial x} \frac{2}{5} \left(\frac{2}{3} a_1^{(i)} + \frac{3}{7} a_3^{(i)} \right) = \mathfrak{J}_2^{(i)}(\underline{a_0}, \underline{a_1}, \underline{a_2}, \underline{a_3}),$$

$$(52) \quad \frac{\partial}{\partial t} \frac{2}{7} a_3^{(i)} + v_i \frac{\partial}{\partial x} \frac{2}{7} \frac{3}{5} a_2^{(i)} = \mathfrak{J}_3^{(i)}(\underline{a_0}, \underline{a_1}, \underline{a_2}, \underline{a_3}).$$

These equations are obtained by exchanging the order of integration and summation as well as by exploiting the orthogonality relations of Legendre polynomials. The collision terms for each Legendre moment λ and speed i are abbreviated by $\mathfrak{J}_\lambda^{(i)}$. We use a vector notation summarizing all speeds of a given Legendre moment λ to $\underline{a_\lambda} = \{a_\lambda^{(0)}, \ldots, a_\lambda^{(n)}\}$.

The collision terms $\mathfrak{J}_\lambda^{(i)}$ are inferred from Eq. (43) by taking into account the

ansatz, Eq. (47), and integrating over the variable θ. They can be cast into the form

$$(53) \qquad \mathcal{J}_\lambda^{(i)} = C_\chi^2 \sum_{j=0}^{n} \sum_{\substack{i+j=h+k}}^{h,k \leq n} v_j \sum_{l,l_*=0}^{N} (\mathcal{G}_{ij}^{hk}(\lambda; l, l_*) \, a_l^{(h)} a_{l_*}^{(k)} - \mathcal{L}_{ij}^{hk}(\lambda; l, l_*) \, a_l^{(i)} a_{l_*}^{(j)}),$$

where the loss terms are given by

$$(54) \qquad \mathcal{L}_{ij}^{hk}(\lambda; l, l_*) = \int_0^\pi \sin\theta \, d\theta \, P_\lambda(\cos\theta) \int_0^{2\pi} d\vartheta \int_{D_{\widehat{\boldsymbol{\Omega}}_*}} d\widehat{\boldsymbol{\Omega}}_* A_{ij}^{hk}(\mu, \vartheta) \, P_l(\cos\theta) \, P_{l_*}(\cos\theta_*),$$

and the gain terms read

$$(55) \qquad \mathcal{G}_{ij}^{hk}(\lambda; l, l_*) = \int_0^\pi \sin\theta \, d\theta \, P_\lambda(\cos\theta) \int_0^{2\pi} d\vartheta \int_{D_{\widehat{\boldsymbol{\Omega}}_*}} d\widehat{\boldsymbol{\Omega}}_* A_{ij}^{hk}(\mu, \vartheta) \, P_l(\cos\theta') \, P_{l_*}(\cos\theta_*').$$

We use the abbreviation $\mu = \cos\beta = \widehat{\boldsymbol{\Omega}} \cdot \widehat{\boldsymbol{\Omega}}_*$.

It is possible to carry out analytically all integrals [64] of the loss term by resorting to an expansion of the collision cross section $A(\mu)$ in Legendre polynomials, which results in

$$(56) \qquad \begin{aligned} \mathcal{L}_{ij}^{hk}(\lambda; l, l_*) &= 2\pi \int_0^\pi \sin\theta \, d\theta \, P_\lambda(\cos\theta) \, P_l(\cos\theta) \, P_{l_*}(\cos\theta) \\ &\times \int_0^{2\pi} d\vartheta \int_{-\mu_0}^{\mu_0} du \, P_{l_*}(\mu) \, A_{ij}^{hk}(\mu, \vartheta). \end{aligned}$$

While the integration over θ can be performed easily, the integral over μ represents the above mentioned expansion of the cross section in Legendre polynomials. The symbol μ_0 stands for $\mu_0 = \min\{1, (v_h v_k)/(v_i v_j)\}$.

Due to the transformation of the argument of the distribution function f to pre-collision velocities, the evaluation of the gain term is more complicated. In fact, it was not possible to carry them out in general analytically but only by means of a numeric quadrature scheme.

It is important to note that not all possible combinations of λ, l, l_* yield nonvanishing loss and gain terms, respectively. Therefore, in the P_3 case we can sim-

plify the collision terms in the following way:

$$(57) \qquad \mathcal{J}_\lambda^{(i)} = C_\chi^2 \sum_{j=0}^{n} \sum_{\substack{i+j=h+k \\ }}^{h,\,k \leqslant n} v_j \sum_{(l,\,l_*)} \left(\mathcal{G}_{ij}^{hk}(\lambda;\,l,\,l_*)\, a_l^{(h)} a_{l_*}^{(k)} - \mathcal{L}_{ij}^{hk}(\lambda;\,l,\,l_*)\, a_l^{(i)} a_{l_*}^{(j)} \right).$$

3.1 - *Macroscopic quantities, moment equations*

In order to obtain the macroscopic quantities of the density ϱ, momentum density ϱu and total kinetic energy density ε of the gas in the P_N approximation, we insert ansatz (47) into the relevant definitions [53]:

$$(58) \quad \varrho = 4\pi m C_\chi \sum_{j=0}^{n} v_j a_0^{(j)}, \quad \varrho u = \frac{4\pi}{3} m C_\chi \sum_{j=0}^{n} v_j^2 a_1^{(j)}, \quad \varepsilon = 2\pi m C_\chi \sum_{j=0}^{n} v_j^3 a_0^{(j)}.$$

The conservation of mass, momentum and energy is expressed by the moment equations derived from Eqs. (49-50). In fact, summing up the evolution equations for the zeroth moment $a_0^{(i)}$, Eq. (49), yields the moment equations for the mass density and energy density:

$$(59) \qquad \frac{\partial \varrho}{\partial t} + \frac{\partial(\varrho u)}{\partial x} = 2\pi m C_\chi \sum_{i=0}^{n} v_i \mathcal{J}_0^{(i)}(\underline{a_0},\, \underline{a_1},\, \underline{a_2},\, \underline{a_3}),$$

$$(60) \qquad \frac{\partial \varepsilon}{\partial t} + \frac{\partial}{\partial x}\left(\frac{2\pi}{3} m C_\chi \sum_{i=0}^{n} v_i^4 a_1^{(i)} \right) = \pi m C_\chi \sum_{i=0}^{n} v_i^3 \mathcal{J}_0^{(i)}(\underline{a_0},\, \underline{a_1},\, \underline{a_2},\, \underline{a_3}),$$

From the evolution of the first Legendre moment $a_1^{(i)}$ as stated in Eq. (50), we infer the evolution of the momentum density:

$$(61) \qquad \frac{\partial(\varrho u)}{\partial t} + \frac{\partial}{\partial x}\left(\frac{2}{3}\varepsilon + \frac{8\pi}{15} m C_\chi \sum_{i=0}^{n} v_i^3 a_2^{(i)} \right) = 2\pi m C_\chi \sum_{i=0}^{n} v_i^2 \mathcal{J}_1^{(i)} \mathcal{J}_0^{(i)}(\underline{a_0},\, \underline{a_1},\, \underline{a_2},\, \underline{a_3}).$$

Due to the knowledge of the explicit form of the gain terms for $\lambda = 0$, conservation of mass and energy can be proven rigorously for arbitrary N [64].

Similar considerations for the collision term of Eq. (61) show that for the conservation of momentum, the following relation is sufficient:

$$(62) \qquad v_h^2 v_k \mathcal{G}_{hk}^{ij}(1, l, l_*) + v_k^2 v_h \mathcal{G}_{kh}^{ji}(1, l_*, l) - v_i^2 v_j \mathcal{L}_{ij}^{hk}(1, l, l_*) - v_j^2 v_i \mathcal{L}_{ji}^{hk}(1, l_*, l) = 0.$$

Since we have no explicit expression for the gain terms $\mathcal{G}_{hk}^{ij}(1,\,l,\,l_*)$, we are not in the position to show rigorously that this is really fulfilled. Numerically, however, this relation is satisfied to high accuracy, i.e. the LHS of Eq. (62) is of the

order $\approx 10^{-23}$ whereas each term in this equation is of the order $\approx 10^{-13}$. Therefore, the moment equations expressing conservation of mass, momentum and energy under the evolution of the P_3 equations are given by

$$(63) \qquad \frac{\partial \varrho}{\partial t} + \frac{\partial (\varrho u)}{\partial x} = 0 \,,$$

$$(64) \qquad \frac{\partial (\varrho u)}{\partial t} + \frac{\partial}{\partial x} \left(\frac{2}{3} \varepsilon + \frac{8\pi}{15} mC_\chi \sum_{j=0}^{n} v_j^3 a_2^{(j)} \right) \approx 0 \,,$$

$$(65) \qquad \frac{\partial \varepsilon}{\partial t} + \frac{\partial}{\partial x} \left(\frac{2\pi}{3} mC_\chi \sum_{j=0}^{n} v_j^4 a_1^{(j)} \right) = 0 \,.$$

4 - Simulations

The P_N multigroup equations are a set of coupled nonlinear partial differential equations. One way of solving them numerically is to resort to an operator splitting method [71]. This approach divides the evolution of the system into a free-streaming part and a collision part within each time step.

An alternative to any operator splitting scheme is the expansion of the spatial dependence of the distribution function f in a Fourier series. This can be done with advantage in the case of cyclic boundary conditions. It has been shown in [60] that this method conserves rigorously mass, momentum and energy. However, care must be taken when tackling the collision terms. Due to their quadratic dependence on f, they introduce high spatial frequencies that must be dropped in a numerical implementation. In order to mitigate the Gibbs oscillations, damping coefficients shall be applied when expanding the initial distribution. A comparison between different approaches to Gibbs damping can be found in [72].

4.1 - *High frequency acoustic waves*

First, we apply the P_1-multigroup equations to a simplified model of the thermal gratings as occurring in degenerate four wave mixing (DFWM) experiments [73]. Two strong coherent laser beams interfere at a small angle within a gas mixture. Their common frequency is tuned as to excite a rare species of the mixture electronically. Within one interval of periodicity of the resulting intensity pattern, called *fringe spacing*, the intensity variations of the laser light follow a cosine-curve. This is due to the two beam interference. Thus, for small laser intensities, the excitation of the rare species has the shape of a cosine within one fringe

spacing. For higher intensities, saturation phenomena alter the shape of this function: The slopes become steeper producing a plateau in the center of the fringe spacing.

The excited species lose their internal energy due to inelastic binary collisions with the dominant species. Thus, kinetic energy and pressure of the gas rise mainly in the center of the fringe spacing. Since this effect occurs periodically according to the interference pattern of the laser beams, a stationary acoustic wave is triggered.

To simulate the evolution of these high frequency density oscillations in the dominant gas, we choose an initial condition of the gas corresponding to the results of these de-excitation processes. Since these oscillations are triggered by a spatially non-homogeneous de-excitation process, the initial condition is not a local Maxwellian. The evolution of the gas is then studied by means of the P_1 multigroup equations.

We choose a spatial interval of $\lambda = 2\pi\mu m$. This is a realistic value for the fringe spacing [73]. To implement the effect of the de-excitation concentrated in the center of the interval, we alter the total thermal equilibrium. Taking into account 16 energy groups, we move particles from the highly occupied low energy groups 1 and 2 to the high energy groups i_0 and $i_0 + 1$ in the tail of the Maxwellian (e.g. $i_0 = 11$). The spatial variation of this initial condition has the shape of a simple cosine function.

To illustrate the departure from thermal equilibrium, Fig. 3 shows the ratio of the distribution function in the center of the fringe spacing to the global Maxwellian. The time evolution is calculated by applying a Fourier expansion in real space [60]. Because of the small Maxwellian tail, one can observe temporal oscillations for high energy groups.

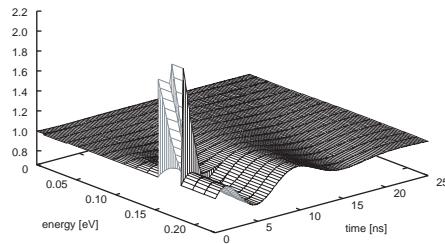When exciting acoustic waves with a two beam interference pattern it may oc-

Fig. 3 - Distribution functions φ_i (i labels the energy groups) divided by the global Maxwellian in the center of the fringe spacing. The peak involving the energy groups $i = 11$ and $i = 12$ at approx. 0.18 eV results from the initial distribution. It relaxes and thus triggers the oscillations.
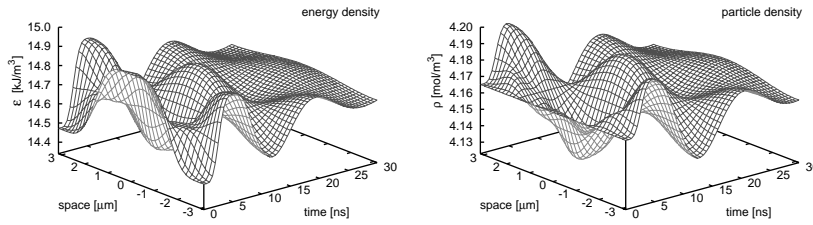
Fig. 4 - Solution of the P_1 equations at $T = 293 \, K$ and $p = 0.1$ bar. The left plot shows the energy variations whereas density variations are plotted in the right graph. The mass and the collision cross section of the gas particles corresponds to that of N_2.

cur that the excitation has not the shape of a simple cosine. This is due to saturation phenomena resulting from the nonlinear reaction of the absorption of the gas for strong intensities. In an extreme case, the initial distribution resembles a rectangular box. The higher spatial frequencies of the initial condition die out very soon leaving a strongly damped stationary acoustic wave. This is illustrated in Figures 4 and 5. We observed no noticeable difference between the results of the operator splitting algorithm and those of the Fourier algorithm.

In the next step we apply the P_3 multigroup equations, Eq. (49-52), to a less simplified model of thermal gratings. We solve the equations numerically by means of the the operator splitting method [71]. The free-streaming time step is approximated by an implicit finite differencing scheme of order 2. The collision time step is carried out on each spatial knot by the application of a Runge Kutta scheme with adaptive step-size control.

The evolution of the high frequency density oscillations of the dominant gas is si-
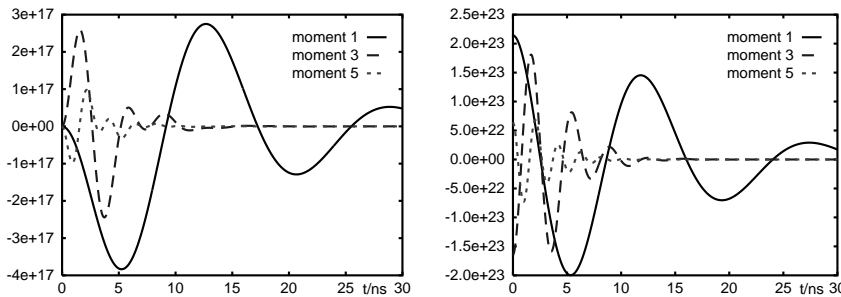

Fig. 5 - Solution of the P_1 equations at $T = 293 \, K$ and $p = 0.1$ bar. The left plot shows the odd cosine-coefficients of the density variations whereas cosine-coefficients of the energy variations are plotted at the RHS. Even coefficients do practically not occur. The amplitude of the third coefficient is multiplied by 5 and that of the fifth coefficient by 25.

energy density —

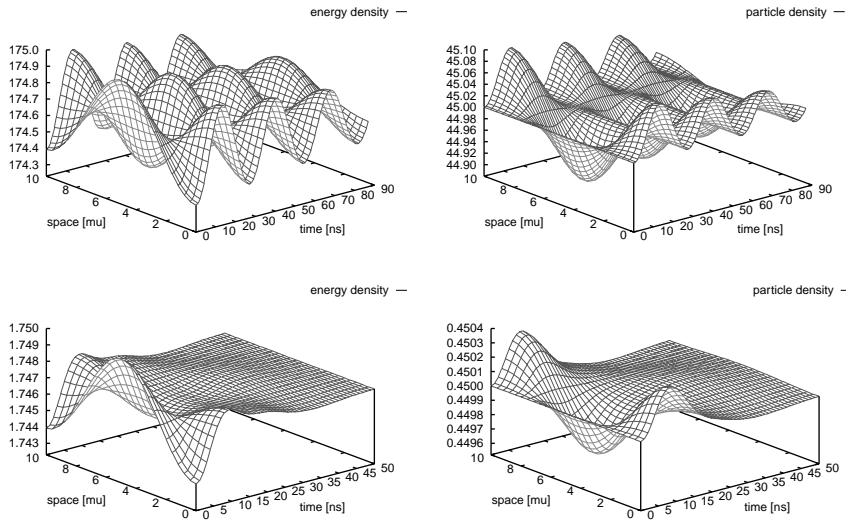particle density —

energy density —

particle density —

Fig. 6 - Oscillations of damped, stationary sound waves generated by two interfering laser beams. The waves are simulated by solving the P_3 multigroup equations within a one-dimensional slab geometry (thickness $10\,\mu$m) for different gas pressures: $p = 1$ bar (on the top) and $p = 0.01$ bar (on the bottom). The pictures on the LHS show the energy density, whereas the pictures on the RHS display the corresponding particle density. The more rarefied the gas is, the stronger the oscillations are damped.

mulated in a one-dimensional slab. The slab thickness is adapted to the fringe spacing given by 10μm. The intensity pattern implies periodic boundary conditions. We choose an initial condition of the gas corresponding to the results of the de-excitation process. Since the oscillations are triggered by a spatially non-homogeneous de-excitation process, the initial condition is not a local Maxwellian. Mainly in the center of the spatial interval, high energy groups are overpopulated.

The evolution of the gas can be split into two phases: At first, local thermal equilibrium is approached within a few nanoseconds due to binary collisions. After that, the collision term virtually vanishes and a damped acoustic wave propagates.

Figure 6 shows the result of such calculations using 13 energy groups for different gas pressures at room temperature $T = 293$ K. We observe that the high energy density in the center of the slab at $t = 0$ leads to a flow of particles to the borders of the slab. It results in a particle depletion in the center, whereas the particle density increases at the borders. This, in turn, increases the energy density and thus the pressure at the borders, which implies a backflow of the gas to the center of the slab. With increasing energy density in the center, the next period of a stationary acoustic wave starts. The more the gas is rarefied, the

higher the Knudsen number is and the more the waves are damped. The speed of sound inferred from the P_3 calculation is $367 \pm 2 \, m/s$ for the case of $p = 1$ bar. This value is in good agreement with the fluid dynamic expectation: the isentropic speed of sound of a monatomic gas is $374 \, m/s$.

4.2 - *Evolution of a hot spot*

In order to show that a P_3 approximation of the semi-continuous Boltzmann equation deals well with hydrodynamic problems, we consider a more pronounced flow problem: the evolution of a hot spot. We choose a spatial interval of length $l = 10$ mm with cyclic boundary conditions and a gas density corresponding to a pressure of $p = 0.1$ bar.

At the beginning of the simulation, the gas of constant density is in local thermal equilibrium in each point of the space interval. We assume, however, a temperature spot exponentially decaying from 352 K in the center to 293 K at the borders of the slab. Figure 7 shows the first 55 μs of the temporal evolution of the energy and particle density and the temperature. At first, the energy peak decreases to a certain amount and propagates to the borders of the slab. Here, the energy density increases in order to be reflected. Then, the two counter propaga-
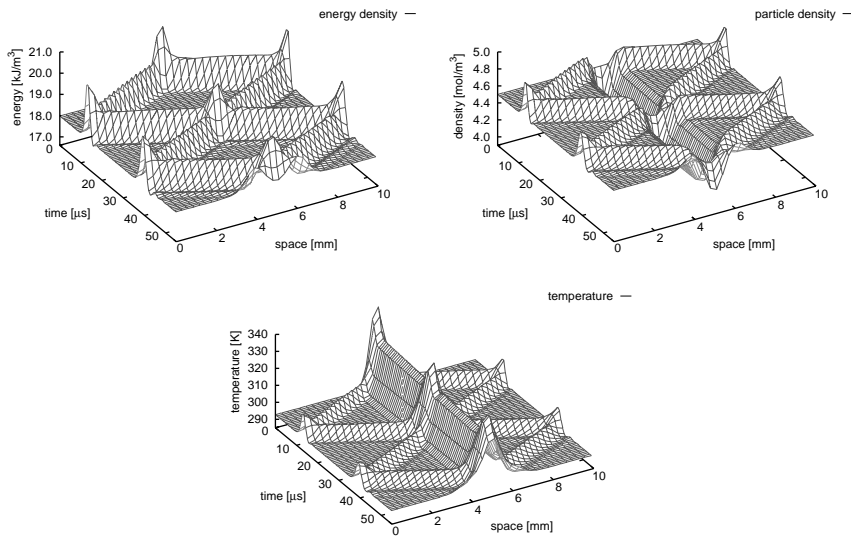
Fig. 7 - Hot spot evolution within a one-dimensional slab. The pictures represent the propagation of the energy and particle density as well as the temperature over the time-space plane.

ting energy density peaks superpose in the center of the slab, where the next cycle starts.

Considering the evolution of the particle density, we notice that this quantity decreases in the center of the slab at first. The reason is the particle flow in direction to the borders triggered by the high energy density in the center of the slab. On the one hand, we observe the propagation of a particle density peak to the borders of the slab and its reflection similar to the propagation of the energy density peaks. On the other hand, we see the continuation of the particle density depletion and the high temperature summit in the center of the slab, only periodically interrupted by the moving particle density and temperature peaks, respectively. It is interesting to note that there are large unaffected parts of the space-time plane during the first few cycles of the evolution. In course of time, however, these flat regions disappear.

4.3 - *Interaction of monochromatic photons with a mixture of gases*

Here we present some numerical results of the extended semi-continuous model. For simplicity, we confine ourselves to the case of a spatially homogeneous and isotropic gas mixture. At this level, we study the impact of a monochromatic laser pulse on the shape of the distribution functions of the gas mixture. The results demonstrate the power and practical usefulness of the model. For the numerical simulations, we implement a P_0 approximation of the semi-continuous kinetic equations.

Apart from the multiplicative constant C_χ, the quantities

$$(66) \qquad n_i^N = v_i \int_{S^2} f_i^N(\widehat{\boldsymbol{\Omega}}) \, d\widehat{\boldsymbol{\Omega}}$$

represent the number of particles N, $N = A$, B and B^*, within the energy group I_i. The evolution equations for the quantities n_i, $\check{n}_i$, $\widehat{n}_i$ and e_R are obtained by integrating Eqs. (26) and (27) with respect to $\widehat{\boldsymbol{\Omega}}$:

$$(67a) \qquad \frac{dn_i}{dt} = \mathcal{Q}_i + Q_i^{AA} + Q_i^{AB} + Q_i^{AB^*},$$

$$(67b) \qquad \frac{d\check{n}_i}{dt} = \check{\mathcal{Q}}_i - \mathcal{S}_i + Q_i^{BB} + Q_i^{BA} + Q_i^{BB^*},$$

$$(67c) \qquad \frac{d\widehat{n}_i}{dt} = \widehat{\mathcal{Q}}_i + \mathcal{S}_i + Q_i^{B^*B^*} + Q_i^{B^*A} + Q_i^{B^*B},$$

$$(67d) \qquad \frac{de_R}{dt} = \frac{d\mathcal{S}_L}{dt} - C_\chi \Delta E \sum_{i=0}^n \mathcal{S}_i.$$

These equations form a set of coupled ordinary differential equations. Here the coupling of the gas particles with the radiation field reads $\mathcal{S}_i = \beta ce_R \check{n}_i - (\alpha + \beta ce_R)\,\widehat{n}_i$ and the integrated collision terms are given by

$$(68a) \qquad \mathcal{Q}_i = \frac{C_\chi^2}{2} \sum_{j=0}^n \left\{ \sum_{\substack{h,k=0 \\ h+k=i+j+q}}^n (\widehat{I}_{hk}^{ij} n_h \check{n}_k - \check{I}_{ij}^{hk} n_i \widehat{n}_j) + \sum_{\substack{h,k=0 \\ h+k=i+j-q}}^n (\check{I}_{hk}^{ij} n_h \widehat{n}_k - \widehat{I}_{ij}^{hk} n_i \check{n}_j) \right\},$$

$$(68b) \qquad \check{\mathcal{Q}}_i = \frac{C_\chi^2}{2} \sum_{j=0}^n \sum_{\substack{h,k=0 \\ h+k=i+j-q}}^n (\check{I}_{hk}^{ij} \widehat{n}_h n_k - \widehat{I}_{ij}^{hk} \check{n}_i n_j),$$

$$(68c) \qquad \check{Q}_i = \frac{C_\chi^2}{2} \sum_{j=0}^n \sum_{\substack{h,k=0 \\ h+k=i+j+q}}^n (\widehat{I}_{hk}^{ij} \check{n}_h n_k - \check{I}_{ij}^{hk} \widehat{n}_i n_j),$$

and

$$(68d) \qquad Q_i^{NM} = \frac{C_\chi^2}{2} \sum_{j=0}^n \sum_{\substack{h,k=0 \\ h+k=i+j}}^n (I_{hk}^{ij} n_h^N n_k^M - I_{ij}^{hk} n_i^N n_j^M).$$

The integrated elastic cross section for Maxwell molecules, e.g., is given by Eqs. (39).

Especially simple expressions for the integrated inelastic cross section are obtained by the choice $\check{\sigma}(g) = d^2 g^+/(4g)$, $\widehat{\sigma}(g) = \Theta(g - \sqrt{2}\varepsilon)\, d^2 g^-/(4g)$ as sketched in Fig. 8 with a hard core of diameter d:

$$(69) \qquad \check{I}_{ij}^{hk} = \frac{2\pi d^2}{v_i v_j} \left(\sqrt{v_i^2 + v_j^2 + 2v_i v_j u_1} - \sqrt{v_i^2 + v_j^2 + 2v_i v_j u_0} \right).$$

Alternatively, the expression for down-scattering $\check{\sigma}(g) = \kappa/g$ corresponding to an up-scattering cross section $\widehat{\sigma}(g) = \kappa\Theta(g - \sqrt{2}\varepsilon)\, g^-/g^2$ is also available analytically:

$$(70) \qquad \check{I}_{ij}^{hk} = \frac{\pi\kappa}{v_i v_j} \arctan\left(\frac{2v_i v_j u - \varepsilon^2}{\sqrt{(v_i^2 + v_j^2)^2 + 2\varepsilon^2(v_i^2 + v_j^2 + 2v_i v_j u) - 4v_i^2 v_j^2 u^2}} \right)\Bigg|_{u_0}^{u_1}.$$
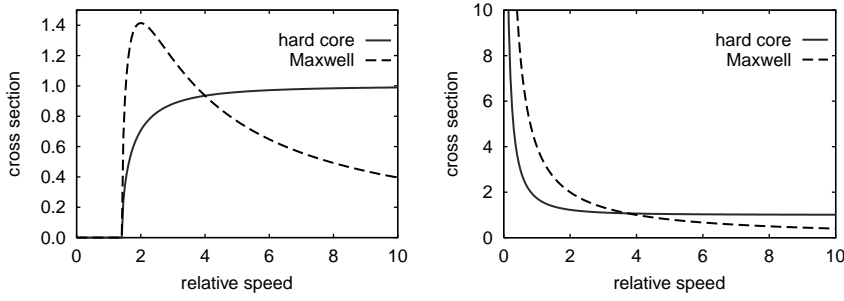
Fig. 8 - Analytic model cross sections for inelastic interactions. The left plot shows excitation and the right plot de-excitation. Speeds are measured in units of ε.

The domain of integration (n_0, n_1) coincide with the bounds of the product $\widehat{\Omega} \cdot \widehat{\Omega}_*$ as given in Eq. (18). The expression for hard sphere down-scattering including elliptic integrals is rather lengthy and shall not be given here.

In order to study relaxation phenomena, Eqs. (67) are solved numerically. Due to the high speed of light $c \approx 3 \cdot 10^8$ m/s, the radiation originating from emission and absorption processes of gas particles is always very close to its equilibrium value. Thus, we approximate it by Planck's law. For the calculation, we fix the following parameters: $\alpha = 10^5 \, \text{s}^{-1}$, $\beta = 10^7 \, \text{m}^2 \, \text{J}^{-1}$, $m = 44$ a.m.u., $n^B + n^{B*} = 2.5 \times 10^{22} \, \text{m}^{-3}$, $\Delta E = 0.27$ eV, $\breve{\sigma}(g) = 5 \times 10^{-17} \, \text{m}^3 \, \text{s}^{-1}/g$. For the dominant species A, we choose three different densities, namely $2.5 \times 10^{23} \, \text{m}^{-3}$ (low density), $2.5 \times 10^{24} \, \text{m}^{-3}$ (medium density), and $2.5 \times 10^{25} \, \text{m}^{-3}$ (high density).

The following scenario is considered: At time $t = 0$, the gas mixture is in thermal equilibrium with the radiation field at temperature $T = 293$ K. Then a laser pulse supplies additional photons. Its intensity is given by the function $I_L(t) = I_0(t/\tau_L) \exp(-(t/\tau_L)^2)$ with $I_0 = 100 \, \text{W/m}^2$ and $\tau_L = 5$ ns. A fraction of these photons is absorbed by species B yielding B^*. The excited particles B^* interact inelastically with particles A in collision de-excitation events (cf. Fig. 10).

The high internal energy released in such a process causes a distortion of the distribution functions. The actual deviation of the particle distribution functions from a Maxwellian depends critically on the assumed cross section and is most pronounced for species B. Figure 9 shows the distribution function of particles B at different instants of time for Maxwell molecules ($\sigma(g) = 5 \times 10^{-17} \, \text{m}^3 \, \text{s}^{-1}/g$) and a low density of particles A (Fig. 10). The deformation can be seen best for $t = 30$ ns.

The equivalent simulation for a hard sphere gas (diameter 3.5 Å) does not show such significant deviations from mechanical equilibrium. The reason is that
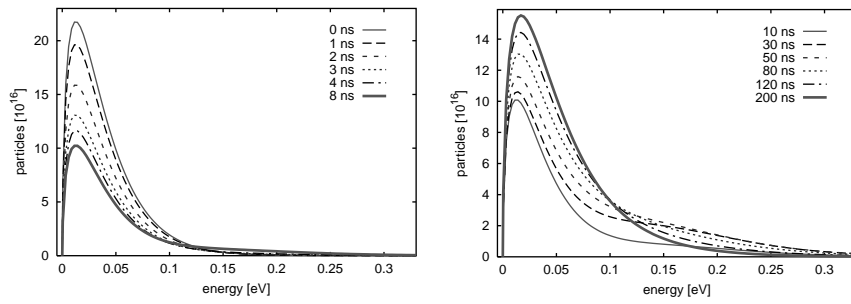
Fig. 9 - Evolution of species B. The left plot shows the first 8 ns where the laser pulse excites the particles and the number of B decreases. The right plot displays the re-appearance of these particles due to inelastic collisions. Note the obvious deviation from a Maxwellian distribution.

for hard sphere particles the collision frequency increases with relative speed and consequently the depletion of the tails is accelerated.

On the other hand, the macroscopic quantities (excitation, energy, kinetic energy) of the gas mixture as depicted in Fig. 11 are relatively unaffected by the choice of the elastic cross section. The curves calculated for hard sphere molecules (HS) virtually coincide with those obtained for Maxwell molecules (MM). The excitation is slightly smaller for hard sphere molecules because of the more efficient Maxwellization of the tails. Consequently, the laser can inject more energy into a hard sphere gas mixture (right column of Fig. 11) as can be seen best for a medium density of species A.

Furthermore, Fig. 11 illustrates how the relaxation behavior depends on the
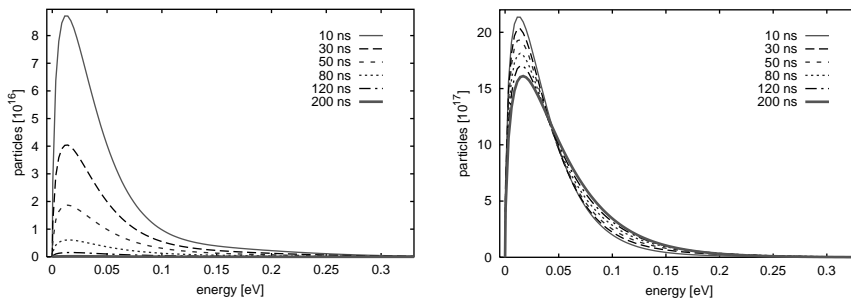
Fig. 10 - Evolution of species B^* (left) and species A (right). Due to de-excitation processes the number density of species B^* decreases in the course of time. The distribution of particles A is shifted towards higher energies as a consequence of the conversion of internal into kinetic energy.
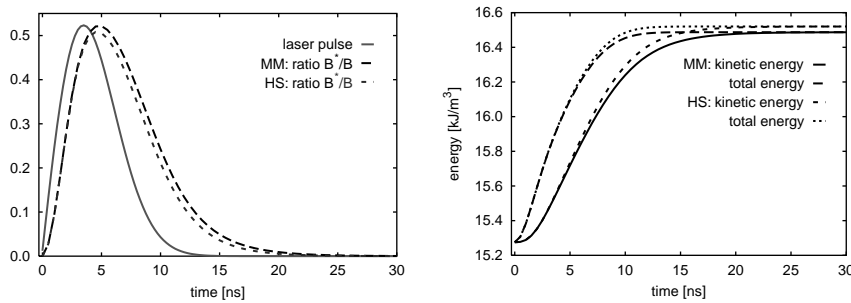
Fig. 11 - Temporal Evolution of macroscopic quantities of the gas mixture for medium density. The left figure shows the excitation (ratio n^{B^*}/n^B) and the intensity of the laser pulse (in arbitrary units) whereas the right one displays the evolution of the kinetic and the total energy density of the gas mixture.

density of particles A: The less particles A the less collision de-excitation events occur per unit time and the greater relaxation times are observed. For the same reason, the excitation (ratio n^{B^*}/n^B) reaches much higher values for low densities of A than for high ones. In the latter case, internal energy is converted to kinetic energy much more efficiently than in the former.

5 - A semi-continuous kinetic model for bimolecular chemical reactions

This section presents a generalization of the semi-continuous kinetic equations to a mixture of four chemically reacting gases. A discussion of the continuous kinetic equations describing the evolution of the gas mixture can be found in [40], [42].

The major new aspect as compared to the previous section is the introduction of different masses of the interacting gas species. This feature gives rise to more complicated expressions for the conservation of momentum and energy already at the level of elastic binary collisions. In the rest of this section, we will denote the four gas species by A, B, C and D, respectively, whereas the letters N and M stand for arbitrary species, $N, M = A, B, C, D$.

For the introduction of the semi-continuous model, we first have to discuss binary collision events involving particles of different masses. After a polar decomposition of the momentum space for any binary collision $N + M \rightleftharpoons N' + M'$, the

conservation of momentum implies the restriction

$$(71) \qquad \frac{1}{2pp_*}((p' - p_*')^2 - p^2 - p_*^2) \leqslant \widehat{\boldsymbol{\Omega}} \cdot \widehat{\boldsymbol{\Omega}}_* \leqslant \frac{1}{2pp_*}((p' + p_*')^2 - p^2 - p_*^2)$$

as a consequence of $-1 \leqslant \widehat{\boldsymbol{\Omega}}' \cdot \widehat{\boldsymbol{\Omega}}_*' \leqslant 1$. Here $p, p_*, \ldots$ denote the moduli and $\widehat{\boldsymbol{\Omega}}, \widehat{\boldsymbol{\Omega}}_*, \ldots$ the direction of the momenta. For a fixed $\widehat{\boldsymbol{\Omega}}$, the set of all $\widehat{\boldsymbol{\Omega}}_*$ satisfying the above condition will be referred to as $D_*(p, p_*, p', p_*')$.

For the purpose of speed-discretization for each species N, we introduce a discrete set of allowed speeds according to

$$(72) \qquad v_i^N = \sqrt{\frac{2}{m^N}\left(E_m + \left(i + \frac{1}{2}\right)\delta\right)},$$

where $n = 0, 1, \ldots, n$, $E_m > 0$ is the minimal kinetic energy and $\delta > 0$ is the size of one energy group. The associated momenta are given by $p_i^N = m^N v_i^N$.

This form of discretization has the advantage of a simple expression for the conservation of energy. In fact, for elastic collisions, energy conservation is expressed by $i + j = h + k$. Moreover, as long as the difference in internal energy Q is given by $Q = q\delta$, $q \in \mathbb{N}$, also the reactive collisions imply $i + j = h + k \pm q$.

We introduce a set of distribution functions $f_i^N(\widehat{\boldsymbol{\Omega}}, \boldsymbol{x}, t)$, $i = 0, 1, \ldots n$ for each species $N = A, B, C, D$. The semi-continuous kinetic equations are obtained by resorting to the discretization procedure of [53] and [64]. They are of the form

$$(73) \qquad \frac{\partial f_i^N}{\partial t} + v_i^N \widehat{\boldsymbol{\Omega}} \cdot \frac{\partial f_i^N}{\partial \boldsymbol{x}} = \mathfrak{J}_i^N + \sum_M J_i^{NM},$$

where J_i^{NM} denotes the influence of elastic collisions between species N and species M on the evolution of the i-th energy group of species N. Similarly, $\mathfrak{J}_i^N$ contains the impact of chemical reactions on the i-th energy group of species N.

First we tackle the problem of elastic collision terms in the semi-continuous theory of the Boltzmann equation. The main problem is to introduce different masses, say mass m^N for species N and mass m^M for species M. The considered interaction reads

$$(74) \qquad N + M \rightleftharpoons N + M.$$

The total mass of the colliding particles is given by $M = m^N + m^M$ whereas the reduced mass and the mass ratio read $\mu^{NM} = m^N m^M / M$ and $r^N = m^N / M$, respectively. In analogy to the formulation given in [53] and [64], the elastic semi-

continuous collision term reads

$$
(75) \quad J_i^{NM}[f^N, f^M] = \frac{\delta^2}{m^M m^N} \sum_{j=0}^{n} v_j^M \sum_{\substack{h,k=0 \\ i+j=h+k}}^{n} \int_0^{2\pi} d\vartheta \int_{D_*(m^N v_i^N,\, m^M v_h^M,\, m^N v_h^N,\, m^M v_k^M)} d\widehat{\boldsymbol{\Omega}}_*
$$

$$
\times \{A_{ij}^{hk}(\widehat{\boldsymbol{\Omega}} \cdot \widehat{\boldsymbol{\Omega}}_*, \vartheta)\}^{NM}[f_{*k}'^M f_h^{N'} - f_{*j}^M f_i^N],
$$

and for the kernel one finds [74]

$$
(76) \quad \{A_{ij}^{hk}(\widehat{\boldsymbol{\Omega}} \cdot \widehat{\boldsymbol{\Omega}}_*, \vartheta)\}^{NM} = \frac{4 m^N}{R}\left(1 + \frac{1}{4}\frac{(m^N - m^M)^2}{m^N m^M}\right)\sigma^{NM}(g, \vartheta),
$$

where $\sigma^{NM} \equiv \sigma^{NM}(g, \vartheta)$ denotes the differential scattering cross section for the elastic interaction, i.e. Eq. (74).

Next, we consider the bimolecular chemical reaction treated in [40], i.e.

$$
(77) \qquad\qquad\qquad A + B \rightleftharpoons C + D - Q,
$$

where $Q > 0$ is the additional internal energy due to stronger chemical bounds of C and D as compared to A and B. We assume that this quantity can be expressed as a multiple of the energy gap δ according to $Q = q\delta$ with $q \in \mathbb{N}$. We introduce the cross section σ_{AB}^{CD} relevant to the chemical reaction and the speeds $g_{NM}^2 = 2Q/\mu^{NM}$. Then the relative speeds after the chemical reaction are given by

$$
(78) \qquad g^- = \sqrt{\frac{\mu^{AB}}{\mu^{CD}}(g^2 - g_{AB}^2)} \quad \text{and} \quad g^+ = \sqrt{\frac{\mu^{CD}}{\mu^{AB}}(g^2 + g_{CD}^2)}
$$

for the endothermic ($\rightarrow$) and the exothermic ($\leftarrow$) direction of the chemical reaction, respectively.

For species A, the semi-continuous collision term for the chemical reaction reads

$$
(79) \quad \mathcal{J}_i^A[f^M] = \frac{\delta^2}{m^B m^C} \sum_{j=0}^{n} v_j^B \sum_{\substack{h,\,k=0 \\ i+j=h+k+q}}^{n} \int_0^{2\pi} d\vartheta \int_{D_*(m^A v_i^A,\, m^B v_j^B,\, m^C v_h^C,\, m^D v_k^D)} d\widehat{\boldsymbol{\Omega}}_*
$$

$$
\times \{\mathcal{C}_{ij}^{hk}(\widehat{\boldsymbol{\Omega}} \cdot \widehat{\boldsymbol{\Omega}}_*, \vartheta)\}^A\left[\left(\frac{m^A m^B}{m^C m^D}\right)^3 f_{*k}'^D f_h^{C'} - f_{*j}^B f_i^A\right],
$$

where, the kernel $\mathcal{A}$ is given by

$$(80) \qquad \{\mathcal{A}_{ij}^{hk}(\widehat{\boldsymbol{\Omega}}\cdot\widehat{\boldsymbol{\Omega}}_*, \vartheta)\}^A = \frac{4gm^C}{g^- R}\left(1 + \frac{1}{4}\frac{(m^D - m^C)^2}{m^C m^D}\right)\sigma_{AB}^{CD}(g, \vartheta).$$

For species B, C and D one obtains similar expressions which can be found in [74].

The obtained semi-continuous transport equations conserve particles, total momentum and total energy [74]. As an impact of the chemical reactions, the individual densities n^N do not remain constant. Only their sum is preserved.

5.1 - *Numerical results*

In this section, some results of the semi-continuous model obtained by an implementation of a P_0 approximation are presented. To this end, we consider a fast exothermic chemical reaction taking place in the mixture of hard sphere particles of diameter $a = 3.46$ Å. The starting point is mechanical (but not chemical) equilibrium of all four species at $T = 300$ K. The initial densities are given by $n^A = 0.0416$ mol/m³, $n^B = 0.00416$ mol/m³, $n^C = 4.16$ mol/m³, $n^D = 41.6$ mol/m³ and the masses are $m^A = 7$, $m^B = 17$, $m^C = 14$ and $m^D = 10$ of the various species. The difference in internal energy is given by $Q = 125$ meV. Chemical reactions are described by $\sigma \sim g^-/g$, and the cross section is chosen 60 times smaller than that for elastic interactions.

Figure 12 shows the evolution of macroscopic quantities during the first 80 ps. Due to the initial rarity of species B, at the beginning, the increase of temperature and particle number is most pronounced for this species. As can be seen in the

Fig. 12 - First few picoseconds of a fast highly exothermic chemical reaction. The left plot shows the evolution of temperature and the right plot the evolution of the densities of the products A and B. In the considered time interval, the densities of the reactants C and D remain virtually constant.
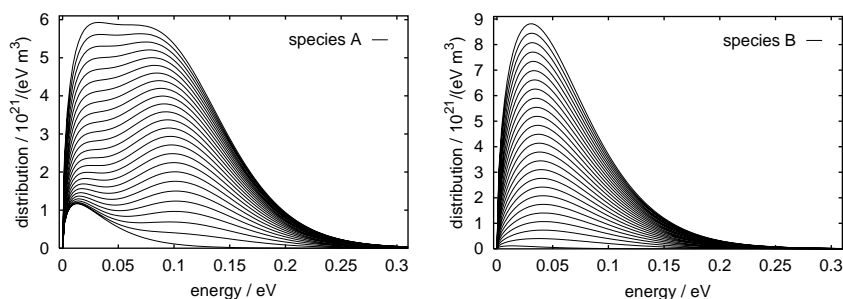
Fig. 13 - First few picoseconds of a fast highly exothermic chemical reaction. The plots show the distribution functions of the products A and B at different instants of time after the ignition of the reaction. The lowest curves show the distribution at $t = 0$ whereas the highest curves correspond to $t = 125$ ps.

right plot of Fig. 12, the number of particles B is 100 times greater at $t = 80$ ps than at the beginning.

During the considered period of time, however, the generated particles A and B undergo very few elastic collisions. For species A additionally, the mass ratio is far from ideal for energy transfer through elastic collisions. Therefore, the products A lose their high kinetic energy very slowly, and their distribution function shows extreme deviations from a Maxwellian. This is illustrated in Fig. 13, which show the distribution functions of the products A and B at different instants of time after the ignition of the reaction. The lowest curves show the distributions at $t = 0$, whereas the highest curves correspond to $t = 125$ ps. On the other hand, the distribution functions of C and D stay virtually constant during the first 80 ns. Due to the non-equilibrium distribution functions of A and also B, the application of the concept of temperature is, of course, highly questionable.

Moreover, Fig. 14 shows the evolution of the temperatures and densities of the various species for the first few nanoseconds of the evolution. We observe that the temperature of the reactants C and D increase to the common limit of about 387. 48 K whereas the products A and B approach the limit from above.

After four nanoseconds, a common temperature is reached and the four particle densities have arrived at constant levels. The final densities of the four species are in excellent agreement with the mass action law [40] that predicts in equilibrium

$$\frac{n^A n^B}{n^C n^D} = \left(\frac{m^A m^B}{m^C m^D} \right)^{3/2} e^{\frac{Q}{k_B T}} = 32.9$$
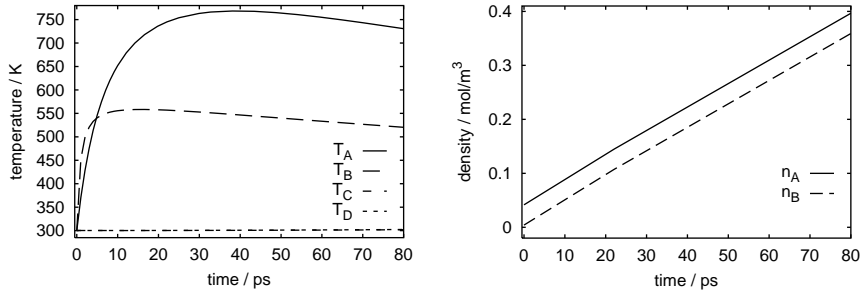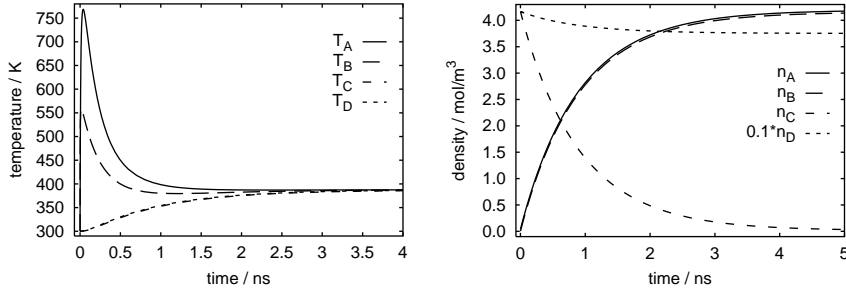
Fig. 14 - First few nanoseconds of a fast highly exothermic chemical reaction. The left plot shows the evolution of temperature and the right plot the evolution of the densities of the various gas species. For convenience, the density of species D is divided by ten.

which has to be compared with the actual value of 32.8 obtained from the numerical results. The discrepancy is less than 0.3 per cent.

Very interesting new features appear as soon as we introduce a threshold for the exothermic direction of the chemical reaction [28]:

$$(81) \qquad \sigma_{AB}^{CD}(g) \sim \frac{1}{g^-}\left(1 - \frac{g_{AB}^2 + g_x^2}{g^2}\right)\Theta(g^2 - (g_{AB}^2 + g_x^2)),$$

where g_x^2 is given by $g_x^2 = 2r\delta/\mu^{AB}$ and r denotes the additional threshold. The dynamics of the reaction depends critically on this threshold r. Depending on the magnitude of the r, we observe a more or less rapid ignition of the reaction.

Two cases are illustrated in Fig. 15, namely the case of a low and a high threshold. For the calculations, the distribution function is resolved using 75 energy groups. The energy gap of the chemical reaction is given by $q = 50 \times \delta$ and the threshold equals $r = 25 \times \delta$. The two different values for the threshold are obtained by modifying the width δ of the energy groups. The values are given by $\delta = 6.25$ and 11.25 meV, respectively. All calculations start at mechanical equilibrium at $T = 300$ K.

For a low value of r, we find that the densities do not decay exponentially to their final values as was the case without exothermic threshold, cf. Fig. 14. As expected, the increasing temperature accelerates the reaction.

For medium and especially very high r, on the other hand, the ignition is delayed for a long time. In the beginning, only a few gas particles react because the gas is still cold. The reactions, however, constantly heat the gas mixture. As soon
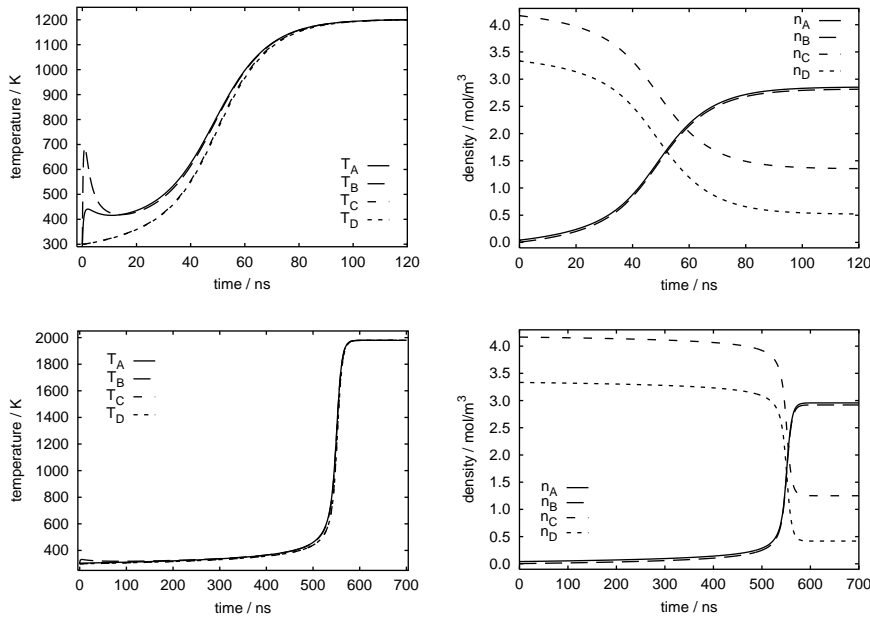
Fig. 15 - Low (top), and high (bottom) threshold.

as the temperature of C and D is high enough, the reaction starts very brutally followed by a rapidly increasing temperature.

6 - Overlapping multigroup approach

In the following sections we present further methods to treat the speed dependence of the distribution function in order to solve the Boltzmann equation. The intention of these alternative approaches is to sustain the smooth character of the velocity distribution. This will allow us to deal with problems where external forces affect the considered gas particles.

Indeed, multigroup discretizations for solving scalar extended Boltzmann equations are not new. A few years ago, the standard multigroup method originally devised for neutron transport was generalized for nonlinear extended kinetic equations [48]. Such an approach, which is the most straightforward application of the method of weighted residuals [75], fits well to the collision term in the linear frame, because it guarantees exact fulfillment of mass conservation at each level of approximation. In fact, when considering the evolution of the test particles, mass is the only quantity conserved under collisions since momentum and energy

are actually exchanged with the field particles. When treating charged particles, the external force term entails derivatives with respect to velocity. The standard procedure [48] eliminates all such derivatives by integration by parts but brings in additional unknowns. In a second step, these quantities must be expressed by suitable interpolation in terms of the actual unknowns and this introduces further approximations.

For this reason, it is preferable to adopt a kind of overlapping multigroup approach [76], which still falls within the method of weighted residuals [75], allowing an exact integration by parts within each group. This is due to the fact that the support of the k-th expansion function consists of two adjacent intervals relevant to the indices k and $k+1$. In addition, different weight functions can be used in combination with the standard one yielding mass conservation. In this way, a better description of the continuous macroscopic balance equations for momentum and energy, although not strictly necessary, is built in the discretized multigroup scheme. In any case, the output for numerical computations is a set of linear integro (with respect to the direction $\widehat{\boldsymbol{\Omega}} = \boldsymbol{v}/v$) differential (with respect to t, $\boldsymbol{x}$ and $\widehat{\boldsymbol{\Omega}}$) equations for the distribution function evaluated at particular speed knots.

The advantage of this approach is that the external force term can be treated in a natural manner avoiding any additional *ad hoc* assumptions. This, however, has to be paid with a more complex structure of the multigroup equations: A matrix appears in front of the time derivative linking the evolution of the various energy groups also on the left hand side of the Boltzmann equation. A refinement of the method sketched in Sec. 8 circumvents this complication by working with orthogonal polynomials.

6.1 - *Extended linear Boltzmann equation*

To demonstrate the overlapping multigroup approach, we consider a linear Boltzmann equation governing the evolution of charged structureless particles scattering inelastically with heavy field particles. External electric and magnetic fields are accounted for. Conservation of mass as well as balance equations for momentum and energy transfer are discussed in the Lorentz gas limit.

For this physical problem the equation governing the evolution of the test particle distribution function reads as [29]

$$(82) \qquad \frac{\partial f}{\partial t} + \boldsymbol{v} \cdot \frac{\partial f}{\partial \boldsymbol{x}} + (\boldsymbol{a} + \boldsymbol{v} \times \boldsymbol{b}) \cdot \frac{\partial f}{\partial \boldsymbol{v}} = C[f],$$

where the collision term on the right hand side $C[f]$ is given by

$$
\begin{aligned}
C[f] = \frac{1}{v} \int d\widehat{\boldsymbol{\Omega}}' \, \{ & n_1 v_+^2 \, \sigma^{12}(v_+, \, \widehat{\boldsymbol{\Omega}} \cdot \widehat{\boldsymbol{\Omega}}') \, f(v_+ \, \widehat{\boldsymbol{\Omega}}') \\
& + n_2 \, \Theta(v^2 - \delta^2) \, v^2 \sigma^{12}(v, \, \widehat{\boldsymbol{\Omega}} \cdot \widehat{\boldsymbol{\Omega}}') \, f(v_- \, \widehat{\boldsymbol{\Omega}}') \\
- f(\boldsymbol{v})[n_1 \, \Theta(v^2 - \delta^2) \, & v^2 \sigma^{12}(v, \, \widehat{\boldsymbol{\Omega}} \cdot \widehat{\boldsymbol{\Omega}}') + n_2 v_+^2 \, \sigma^{12}(v_+, \, \widehat{\boldsymbol{\Omega}} \cdot \widehat{\boldsymbol{\Omega}}')] \} \, .
\end{aligned}
$$

(83)

The integration on the right hand side extends over the two-dimensional unit sphere S^2. Here, U denotes the unit step function and $\widehat{\boldsymbol{\Omega}}$, $\widehat{\boldsymbol{\Omega}}'$ are unit vectors in the velocity space such that the polar decomposition of the velocity vector $\boldsymbol{v}$ is given by $v\widehat{\boldsymbol{\Omega}}$ with $v = |\boldsymbol{v}|$. To simplify notation, the dependence on $\boldsymbol{x}$ and t is not explicitly shown, unless necessary. Furthermore, we have introduced the abbreviations

$$
\text{(84)} \qquad v_\pm = \sqrt{v^2 \pm \delta^2} \, , \qquad \delta^2 = \frac{2\Delta E}{m} \, , \qquad \boldsymbol{a} = q\boldsymbol{E}/m \, , \qquad \boldsymbol{b} = q\boldsymbol{B}/m \, .
$$

For simplicity, only constant external electric ($\boldsymbol{E}$) and magnetic ($\boldsymbol{B}$) fields will be considered. Field particles are taken to be in equilibrium at zero drift velocity and temperature T, with number densities n_1 and n_2 for the fundamental and excited species B_1 and B_2, respectively. All quantities are assumed to be constant versus $\boldsymbol{x}$ and t. In thermal equilibrium, the densities n_1 and n_2 are related by the Boltzmann factor

$$
\text{(85)} \qquad \frac{n_2}{n_1} = \exp\left(- \frac{\Delta E}{k_B T} \right),
$$

where $\Delta E = E_2 - E_1 > 0$ is the difference between the energy levels of species B and k_B denotes the Boltzmann constant.

The cross section σ^{12} refers to the scattering collision which transforms species B_1 into B_2; the other cross section σ^{21} for the de-excitation process has been eliminated by means of the microreversibility condition

$$
\text{(86)} \qquad v^2 \sigma^{12}(v, \, \widehat{\boldsymbol{\Omega}} \cdot \widehat{\boldsymbol{\Omega}}') = \Theta(v^2 - \delta^2) \, v_-^2 \, \sigma^{21}(v_-, \, \widehat{\boldsymbol{\Omega}} \cdot \widehat{\boldsymbol{\Omega}}') \, .
$$

One can easily recognize the four addends making up the collision integral: The gain term contributed by down-scattering, the gain term due to up-scattering and the corresponding two loss terms, respectively. Of course, any excitation (de-excitation) process corresponds to decreasing (increasing) the test particle's quadratic speed by δ^2. The step function Θ accounts for the relevant thresholds. In view of

the planned speed discretization, it is useful to split the velocity gradient as

$$(87) \qquad \frac{\partial f}{\partial \boldsymbol{v}} = \widehat{\boldsymbol{\Omega}} \, \frac{\partial f}{\partial v} + \frac{1}{v} \, \frac{\partial f}{\partial \widehat{\boldsymbol{\Omega}}} \, .$$

The properties of the collision term $C[f]$ are discussed in [32]. For the purpose of this paper, it is sufficient to note that it guarantees mass conservation, i.e.

$$(88) \qquad \int\limits_0^\infty v^2 \, dv \int C[f] \, d\widehat{\boldsymbol{\Omega}} = 0 \qquad \text{for all } f,$$

and that collision equilibria are exhausted by the class of functions

$$(89) \qquad f(v\widehat{\boldsymbol{\Omega}}) = \Gamma(v^2) \exp\left(- \frac{mv^2}{2k_B T}\right) \qquad \text{with } \Gamma(\delta^2 + v^2) = \Gamma(v^2).$$

These equilibria are a Maxwellian at the background drift velocity and temperature times any periodic function of v^2 with period δ^2/k, $k \in \mathbb{N}$.

We shall confine ourselves to small spatial gradients and small fields. This allows a treatment of the angle variable $\widehat{\boldsymbol{\Omega}}$ by resorting to the lowest order truncated spherical harmonics expansion (P_1-*approximation*). Of course, the considerable simplification achieved has a counterpart in the loss of generality associated to the restricted range of validity of a linear anisotropy approximation for the distribution function.

In the rest of this section, we shall drop the superscript 12 from the cross section since the inverse cross section will not be needed.

6.2 - *Overlapping multigroup approach*

The strategy of the approach is the following: After discretizing the speed variable v, we introduce shape functions $\chi(v)$ bearing the v dependence of the distribution function f within each energy group. Subsequently, we multiply the Boltzmann equation by the non-negative weight functions v^l, $l = 2, 3, \ldots$. We then obtain moment equations by integrating the weighted Boltzmann equation with respect to v over the various energy groups. These moment equations are shown to conserve the number of test particles.

For the introduction of energy groups, we consider a partition of the non-negative real axis $v \in (0, +\infty)$ in terms of N intervals located between the $N + 1$ knots w_i, $i = 0, 1, \ldots, N$ (starting from $w_0 = 0$). The number N has to be large

enough, so that the distribution function evaluated at the final knot, $f(w_N \widehat{\boldsymbol{\Omega}})$, can be considered negligible. Introducing $f_i(\widehat{\boldsymbol{\Omega}}) \equiv f(w_i \widehat{\boldsymbol{\Omega}})$ as the new unknowns entails that only N nonvanishing functions are left. The physical problem suggests the following choice:

$$w_0 = 0, \quad w_{i+1} = \sqrt{w_i^2 + \varepsilon}, \qquad \text{with} \qquad \varepsilon = \delta^2 = 2\Delta E/m .$$

As in each weighted residuals method, we introduce N non-negative continuous basis functions $\chi_i(v)$, $i = 0, 1, \ldots, N-1$. In particular, we choose them in such a way that they meet the requirements

$$\chi_i(v) = 0 \quad \text{for } v \leqslant w_{i-1} \quad \text{and} \quad i > 0$$

$$\chi_i(w_i) = 1$$

$$\chi_i(v) = 0 \quad \text{for } v \geqslant w_{i+1}.$$

Remark 1. It is also possible to work with an adimensionalized system of equations by using v^2 as new independent variable and measuring it in units of $2\Delta E/m$. This has the consequence that the knots are equally spaced and located at integer numbers. ■

For the purpose of the multigroup approach, we make the usual assumption of separability. Therefore, the function $f(v\widehat{\boldsymbol{\Omega}})$ is approximated by

$$(90) \qquad\qquad f(v\widehat{\boldsymbol{\Omega}}) = \sum_{i=0}^{N-1} f(w_i \widehat{\boldsymbol{\Omega}}) \, \chi_i(v) .$$

The assumption of linear and continuous functions χ_i on the intervals $[w_{i-1}, w_i]$ and $[w_{i-1}, w_i]$ (i.e. tent functions) is equivalent to the linear interpolation of $f(v)$ between the knots.

Remark 2. Since the ansatz of Eq. (90) provides values of f for each speed v, it implicitly rules out any arbitrariness of the equilibrium distribution as stated in Eq. (89). Notice, however, that this arbitrariness also disappears physically as soon as we apply an external field. In this case, each velocity $\boldsymbol{v}$ is related to all other velocities by the streaming term of the Boltzmann equation. ■

A system of equations for the unknowns $f_k(\widehat{\boldsymbol{\Omega}})$ is constructed by multiplying the linear kinetic equation Eq. (82) by some weight function $\psi(v)$ and integrating over the intervals $v \in [w_k, w_{k+1}]$ for $k = 0, 1, \ldots, N-1$. The original multigroup method [48] corresponds to the option $\psi(v) = v^2$ on all intervals, which guarantees exact fulfillment of mass conservation. This choice remains appropriate here,

but, for the sake of generality, we will take as weight function an arbitrary power of v, say v^l, with integer l.

For a general $l \geq 2$, the system of N multigroup equations can be written as

$$
\begin{aligned}
(91) \quad & \frac{\partial}{\partial t}(f_k \mathfrak{I}_k^{(l)} + f_{k+1} \mathfrak{J}_k^{(l)}) + \widehat{\boldsymbol{\Omega}} \cdot \nabla (f_k \mathfrak{I}_k^{(l+1)} + f_{k+1} \mathfrak{J}_k^{(l+1)}) \\
& + \boldsymbol{a} \cdot \widehat{\boldsymbol{\Omega}}[w_{k+1}^l f_{k+1} - w_k^l f_k - l(f_k \mathfrak{I}_k^{(l-1)} + f_{k+1} \mathfrak{J}_k^{(l-1)})] \\
& + \boldsymbol{a} \cdot \frac{\partial}{\partial \widehat{\boldsymbol{\Omega}}}(f_k \mathfrak{I}_k^{(l-1)} + f_{k+1} \mathfrak{J}_k^{(l-1)}) + (\widehat{\boldsymbol{\Omega}} \times \boldsymbol{b}) \cdot \frac{\partial}{\partial \widehat{\boldsymbol{\Omega}}}(f_k \mathfrak{I}_k^{(l)} + f_{k+1} \mathfrak{J}_k^{(l)}) \\
& = n_1 \int d\widehat{\boldsymbol{\Omega}}' \, [f_{k+1}(\widehat{\boldsymbol{\Omega}}') \, \mathcal{G}_{k,k+1}^{(l-1)}(\widehat{\boldsymbol{\Omega}} \cdot \widehat{\boldsymbol{\Omega}}') + f_{k+2}(\widehat{\boldsymbol{\Omega}}') \, \mathcal{G}_{k,k+2}^{(l-1)}(\widehat{\boldsymbol{\Omega}} \cdot \widehat{\boldsymbol{\Omega}}')] \\
& + \not{\delta}_{k,0} n_2 \int d\widehat{\boldsymbol{\Omega}}' \, [f_{k-1}(\widehat{\boldsymbol{\Omega}}') \, \mathcal{G}_{k,k-1}^{(l-1)*}(\widehat{\boldsymbol{\Omega}} \cdot \widehat{\boldsymbol{\Omega}}') + f_k(\widehat{\boldsymbol{\Omega}}') \, \mathcal{G}_{k,k}^{(l-1)*}(\widehat{\boldsymbol{\Omega}} \cdot \widehat{\boldsymbol{\Omega}}')] \\
& - \not{\delta}_{k,0} n_1 (\mathcal{L}_{k,k}^{(l-1)} f_k + \mathcal{L}_{k,k+1}^{(l-1)} f_{k+1}) - \not{\delta}_{k,N-1} n_2 (\mathcal{L}_{k,k}^{(l-1)*} f_k + \mathcal{L}_{k,k+1}^{(l-1)*} f_{k+1}),
\end{aligned}
$$

where we have used the abbreviations

$$
(92) \qquad \mathfrak{I}_k^{(l)} = \int_{w_k}^{w_{k+1}} \chi_k(v) \, v^l \, dv \quad \text{and} \quad \mathfrak{J}_k^{(l)} = \int_{w_k}^{w_{k+1}} \chi_{k+1}(v) \, v^l \, dv .
$$

It should be noted that different power moments of the basis functions χ_i are needed for a consistent approximation of different macroscopic quantities. The index k ranges from $k = 0, 1, \ldots, N-1$. The integral $\int d\mu$ is always extended over the interval $[-1, +1]$. In addition to the complementary Kronecker delta $\not{\delta}_{k,l} = 1 - \delta_{k,l}$, we have introduced the following new symbols:

$$
(93a) \qquad \mathcal{G}_{k,i}^{(l)}(\mu) = \int_{w_k}^{w_{k+1}} v^l \, dv [v_+^2 \, \sigma(v_+, \mu) \, \chi_i(v_+)],
$$

$$
(93b) \qquad \mathcal{G}_{k,i}^{*(l)}(\mu) = \int_{w_k}^{w_{k+1}} v^l \, dv [v^2 \, \sigma(v, \mu) \, \chi_i(v_-)],
$$

$$
(93c) \qquad \mathcal{L}_{k,i}^{(l)} = \int_{w_k}^{w_{k+1}} v^l \, dv \int 2\pi d\mu [v^2 \, \sigma(v, \mu) \, \chi_i(v)],
$$

$$
(93d) \qquad \mathcal{L}_{k,i}^{*(l)} = \int_{w_k}^{w_{k+1}} v^l \, dv \int 2\pi d\mu [v_+^2 \, \sigma(v_+, \mu) \, \chi_i(v)].
$$

As stated above, the choice $l = 2$ yields a valid algorithm for numerical implementation, even though we miss the powers v^3 and v^4 needed to accurately describe the evolution of momentum and energy density.

We construct a consistent and closed set of multigroup equations in the following way. We choose an integer number L and consider Eq. (91) for all $l = 2, \ldots, L$. This yields a system of $(L-1) \times N$ equations for the N unknowns $f_0, \ldots, f_{N-1}$, which is, except for $L = 2$, overdetermined. This overdetermination is cured by adding $L-1$ neighboring equations (with respect to k) to obtain one new equation. For this reason, N must be chosen as a multiple of $L-1$, and $N/(L-1)$ equations are obtained for each value of l.

Remark 3.   This procedure is equivalent to integrating over intervals of the length $(L-1)\,\Delta E$ in energy space. For $L \geqslant 4$ not only mass conservation, but also momentum and energy balance are adequately accounted for. In any case, the unknowns f_k are representative for the energy groups and come from a weighting procedure over energy intervals of length ΔE or multiples thereof.   ∎

6.3 - *Numerical treatment*

By formulating an overlapping multigroup approach in Eq. (91), we have treated the speed variable of the distribution function. With respect to the direction $\widehat{\boldsymbol{\Omega}}$ of the velocity, Eq. (91) is still of integro-differential type. In the next step, one has to reduce the system of multigroup equations to a system of linear partial differential equations with respect to time t and space $\boldsymbol{x}$.

If both the spatial gradients and the electric field are small, we can achieve our aim of reducing the integro-differential equation, Eq. (91), to a differential equation by resorting to a truncated spherical harmonic expansion of $f_k(\widehat{\boldsymbol{\Omega}})$. Up to the first order, our ansatz for $f(\widehat{\boldsymbol{\Omega}})$ reads

$$(94) \qquad\qquad f_k(\widehat{\boldsymbol{\Omega}}) = \frac{1}{4\pi}\,(N_k + 3\,\widehat{\boldsymbol{\Omega}}\cdot\boldsymbol{J}_k)\,,$$

where the symbols appearing in this definition are defined as

$$N_k = \int f_k(\widehat{\boldsymbol{\Omega}})\,d\widehat{\boldsymbol{\Omega}}, \qquad \boldsymbol{J}_k = \int \widehat{\boldsymbol{\Omega}} f_k(\widehat{\boldsymbol{\Omega}})\,d\widehat{\boldsymbol{\Omega}}.$$

In order to simplify notation, we work with a coordinate system whose z axis coincides with the direction of the electric field. Furthermore, we rotate the coordinate system in such a way that the x component of the magnetic flux vanishes. Therefore, we can write

$$(95) \qquad\qquad \boldsymbol{a} = (0, 0, a)^{\dagger} \quad \text{and} \quad \boldsymbol{b} = (0, \mathrm{b_y}, \mathrm{b_z})^{\dagger}.$$

The resulting P_1 overlapping multigroup equations can be cast after some algebra as shown in [77] in a matrix form:

(96)
$$\frac{\partial}{\partial t} \begin{pmatrix} N \\ J^z \\ J^x \\ J^y \end{pmatrix} = \begin{bmatrix} C & -aB & 0 & 0 \\ -aD/3 & F & b_y E & 0 \\ 0 & -b_y E & F & b_z E \\ 0 & 0 & -b_z E & F \end{bmatrix} \begin{pmatrix} N \\ J^z \\ J^x \\ J^y \end{pmatrix},$$

where E stands for the unit matrix. We now write N, J^z, J^x and J^y for the N-tuples $(N_0, \ldots, N_{N-1})^\dagger$, $\ldots$, respectively. For crossed fields, i.e. $b_z = 0$, the equation for J^y is not needed.

As the easiest test case, we illustrate the relaxation of an isotropic non-equilibrium distribution to a Maxwellian. Its temperature is imposed by the field particles. Due to the special distortion of the initial distribution function, the kinetic energy of the test particles first increases to a maximum and then slowly decreases to its equilibrium value. The 3d plot of Fig. 16 gives an impressive appreciation of the actual departure from equilibrium. It shows the ratio of the distribution function divided by the final Maxwellian versus speed and time.

Next we study the impact of an electric field on the distribution function f. According to the results obtained by a Fokker-Planck approximation [43], [78] for $\Delta E \ll 3 k_B T/2$, this impact depends on the interaction law. It is, of course, much stronger for the $1/v$ decreasing cross section of Maxwell molecules than for hard spheres, where the cross section is constant versus v. Figure 17 shows the isotropic part of the distribution function divided by the Maxwellian versus speed and time. At time $t = 1000$ the electric field is turned on and begins to act on the initial distribution which is a Maxwellian with the temperature of the background gas.

It should be noted that the differently strong fields induce an almost equal distortion of the distribution function for high speeds. For low speeds, however, the
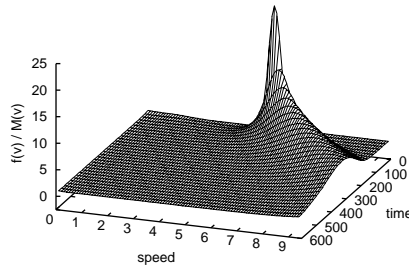
Fig. 16 - Relaxation to a Maxwellian. The plot shows the distribution function N_k versus speed and time divided by the Maxwellian.
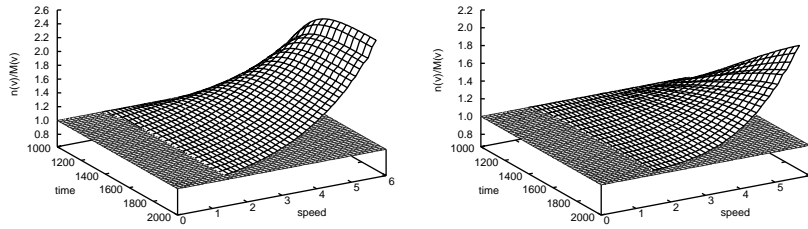
Fig. 17 - Ratio density distribution function/Maxwellian versus speed and time. A field of a = 2.5 a.u. acts on the hard sphere test particles (left plot) whereas a field of $a = 0.6$ a.u. acts on the Maxwell test particles (right plot).
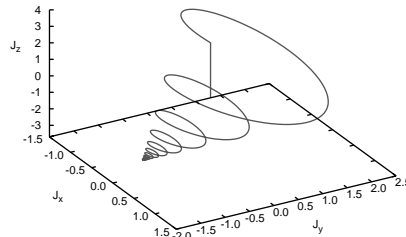
Fig. 18 - 3d plot J_x versus J_y and J_z. The straight line joining the point $(0, 0, 4)$ with the origin is due to the application of the electric field only. After changing the sign of the electric field, the current J_z also changes its sign. Because of the additional magnetic field, the phase trajectory has the form of a spiral.

cross section of Maxwellian molecules tends to infinity. Therefore, the distribution function is only very slightly below unity as compared to the case of hard sphere particles.

Next, we introduce an external electric field giving rise to a current, and in a further step we add a magnetic field acting on this current. Thus, we obtain a simple, spatially homogeneous kinetic model of the *Hall effect*. If we change the sign of the electric field and simultaneously apply the magnetic field in both directions, y and z, we obtain the most interesting behavior of such a model: When plotting the (J_x, J_y, J_z) projection of the phase space, we find a spiral on a cone. This phenomenon can be seen in Fig. 18.

7 - Linear spline interpolation

The overlapping multigroup approximation as described in Sec. **6** represents a first approach to incorporate external fields in a discretization of a linear Bol-

tzmann transport equation. Although meeting the major physical requirements (conservation of particles, balance of momentum and energy), this method turns out to work well only for small electric fields. Numerical instabilities are found to spoil the algorithm by inducing heavy and unphysical oscillations of the distribution function. This happens predominantly as soon as one tries to simulate the impact of higher electric fields.

Here, we therefore present a more stable generalization of the overlapping multigroup approach. Instead of working with rigid shape functions, we resort to a *spline approximation* of the speed-dependence of the distribution function. External fields can be naturally included in this multigroup scheme.

The method presented here has the advantage of great flexibility. The degree of smoothness of the distribution function can be controlled by means of a certain number of continuity conditions. Furthermore, in this way, one obtains many more equations per speed interval (in fact, as many as one wants to deal with) than in the former approach and thus increases the accuracy of the approximation. Finally, the original overlapping multigroup method can be recovered as a special case of the spline multigroup approach.

7.1 - *Multigroup equations*

For convenience, we absorb the factor v^2 in the definition of the distribution function and resort to a polar decomposition of the velocity variable $\boldsymbol{v} = v\widehat{\boldsymbol{\Omega}}$, where $v = |\boldsymbol{v}|$ and $\widehat{\boldsymbol{\Omega}} = \boldsymbol{v}/v$. In terms of the new dependent variable $\varphi(v, \widehat{\boldsymbol{\Omega}}) = v^2 f(v\widehat{\boldsymbol{\Omega}})$, where $f(\boldsymbol{v}, \boldsymbol{x}, t)$ stands for the phase density of particles A, the Boltzmann equation reads

$$(97) \quad \frac{\partial \varphi}{\partial t} + v\widehat{\boldsymbol{\Omega}} \cdot \frac{\partial \varphi}{\partial \boldsymbol{x}} + \boldsymbol{a} \cdot \left[\left(-\frac{2}{v}\varphi + \frac{\partial \varphi}{\partial v} \right) \widehat{\boldsymbol{\Omega}} + \frac{1}{v} \frac{\partial \varphi}{\partial \widehat{\boldsymbol{\Omega}}} \right] + (\widehat{\boldsymbol{\Omega}} \times \boldsymbol{b}) \cdot \frac{\partial \varphi}{\partial \widehat{\boldsymbol{\Omega}}} = C[\varphi].$$

In the case of a Lorentz gas where (test) particles A collide inelastically with heavy field particles B, i.e., the model described in the previous section, the linear collision operator C describing the interaction $A + B_1 \rightleftharpoons A + B_2$ is given by

$$(98) \quad C[\varphi] = \frac{1}{v} \int d\widehat{\boldsymbol{\Omega}}' \left\{ n_1 v^2 \sigma(v_+, \widehat{\boldsymbol{\Omega}}' \cdot \widehat{\boldsymbol{\Omega}}) \, \varphi(v_+, \widehat{\boldsymbol{\Omega}}') + n_2 \frac{v^4}{v_-^2} \sigma(v, \widehat{\boldsymbol{\Omega}}' \cdot \widehat{\boldsymbol{\Omega}}) \, \varphi(v_-, \widehat{\boldsymbol{\Omega}}') \right.$$

$$\left. - \varphi(v)[n_1 v^2 \sigma(v, \widehat{\boldsymbol{\Omega}}' \cdot \widehat{\boldsymbol{\Omega}}) + n_2 v_+^2 \sigma(v_+, \widehat{\boldsymbol{\Omega}}' \cdot \widehat{\boldsymbol{\Omega}}) \right\}.$$

The density of B_1 (ground state of B) and B_2 (excited state of B) is denoted by n_1

and n_2, respectively. The cross section σ controls the rate of the above mentioned interaction (excitation of B).

The positive real axis of speeds is partitioned in terms of N intervals located between the $N + 1$ knots $w_0 = 0 < w_1 < \ldots < w_N$. Henceforth it shall be assumed that the influence of particles of speed higher than w_N is negligible. On each interval $I_\nu = [w_{\nu-1}, w_\nu)$, the distribution function is approximated by a polynomial of degree Λ. The dependence on v and on $\widehat{\boldsymbol{\Omega}}$ is separated by the ansatz

$$(99) \qquad \varphi(v, \widehat{\boldsymbol{\Omega}}) = \sum_{\nu=1}^{N} \varphi_\nu(v, \widehat{\boldsymbol{\Omega}}) = \sum_{\nu=1}^{N} \sum_{\lambda=0}^{\Lambda} \varphi_\nu^{(\lambda)}(\widehat{\boldsymbol{\Omega}}) \, \chi_{I_\nu}(v) \, (v - w_{\nu-1})^\lambda,$$

where χ_B stands for the characteristic function of the set B and $\varphi_\nu(v, \widehat{\boldsymbol{\Omega}})$ is the restriction of the distribution function φ to the interval I_ν. The $(\Lambda + 1) \times N$ unknowns $\varphi_\nu^{(\lambda)}$ depend on space $\boldsymbol{x}$, time t and the angle $\widehat{\boldsymbol{\Omega}}$. Thus the same number of equations is needed. Part of them stem from the requirement of continuity of φ at the speed knots w_ν,

$$\varphi_\nu(w_\nu, \widehat{\boldsymbol{\Omega}}) = \varphi_{\nu+1}(w_\nu, \widehat{\boldsymbol{\Omega}}),$$

$$(100) \qquad \varphi_\nu'(w_\nu, \widehat{\boldsymbol{\Omega}}) = \varphi_{\nu+1}'(w_\nu, \widehat{\boldsymbol{\Omega}}),$$

$$\vdots \qquad\qquad\qquad\qquad \nu = 1, \ldots, N-1,$$

$$\frac{\partial^M}{\partial v^M} \varphi_\nu(w_\nu, \widehat{\boldsymbol{\Omega}}) = \frac{\partial^M}{\partial v^M} \varphi_{\nu+1}(w_\nu, \widehat{\boldsymbol{\Omega}}),$$

where primes refer to derivatives with respect to v. This yields a set of $(N-1) \times (M+1)$ equations. Combined with the natural and physically meaningful boundary conditions

$$\varphi_1(0, \widehat{\boldsymbol{\Omega}}) = \varphi_1'(0, \widehat{\boldsymbol{\Omega}}) = 0,$$

$$(101) \qquad \varphi_N''(w_N, \widehat{\boldsymbol{\Omega}}) = \ldots = \frac{\partial^M}{\partial v^M} \varphi_N(w_N, \widehat{\boldsymbol{\Omega}}) = 0,$$

we obtain a set of $(M+1) \times N$ equations. In terms of the new unknowns $\varphi_\nu^{(\lambda)}(\widehat{\boldsymbol{\Omega}})$, the boundary conditions read

$$\varphi_1^{(0)}(\widehat{\boldsymbol{\Omega}}) = \varphi_1^{(1)}(\widehat{\boldsymbol{\Omega}}) = 0,$$

$$(102) \qquad \sum_{\lambda=m}^{\Lambda} \binom{\lambda}{m} (w_N - w_{N-1})^{\lambda-m} \varphi_N^{(\lambda)}(\widehat{\boldsymbol{\Omega}}) = 0, \qquad m = 2, \ldots, M.$$

The continuity conditions are of the form

$$\sum_{\lambda=0}^{\Lambda} (w_\nu - w_{\nu-1})^\lambda \, \varphi_\nu^{(\lambda)}(\widehat{\boldsymbol{\Omega}}) = \varphi_{\nu+1}^{(0)}(\widehat{\boldsymbol{\Omega}}),$$

(103) $$\sum_{\lambda=1}^{\Lambda} \lambda (w_\nu - w_{\nu-1})^{\lambda-1} \, \varphi_\nu^{(\lambda)}(\widehat{\boldsymbol{\Omega}}) = \varphi_{\nu+1}^{(1)}(\widehat{\boldsymbol{\Omega}}),$$

$$\vdots \qquad\qquad\qquad\qquad\qquad \nu = 1, \, \dots, \, N-1 ,$$

$$\sum_{\lambda=M}^{\Lambda} \binom{\lambda}{M} (w_\nu - w_{\nu-1})^{\lambda-M} \, \varphi_\nu^{(\lambda)}(\widehat{\boldsymbol{\Omega}}) = \varphi_{\nu+1}^{(M)}(\widehat{\boldsymbol{\Omega}}).$$

The other equations are, of course, obtained from the linear Boltzmann equation. To this end, Eq. (97) is multiplied by the weights v^l, for $l = 0, 1, \dots, L$ and integrated over the intervals I_ν. This procedure yields a set of $(L+1) \times N$ *spline-multigroup* equations. For the Lorentz gas model with inelastic scattering, these equations take on their simplest form if the speed knots are chosen as $w_i^2 = i\delta^2$ with $i = 0, 1, \dots, N$ and $\delta^2 = 2\Delta E/m$. In this case we find

(104)
$$\sum_{\lambda=0}^{\Lambda} \left\{ \langle v^l \rangle_{\nu,\lambda} \, \frac{\partial}{\partial t} \, \varphi_\nu^{(\lambda)}(\widehat{\boldsymbol{\Omega}}) + \langle v^{l+1} \rangle_{\nu,\lambda} \, \widehat{\boldsymbol{\Omega}} \cdot \frac{\partial}{\partial \boldsymbol{x}} \, \varphi_\nu^{(\lambda)}(\widehat{\boldsymbol{\Omega}}) \right.$$

$$+ \langle v^{l-1} \rangle_{\nu,\lambda} \, \boldsymbol{a} \cdot \left[-2 \, \widehat{\boldsymbol{\Omega}} \, \varphi_\nu^{(\lambda)}(\widehat{\boldsymbol{\Omega}}) + \frac{\partial}{\partial \widehat{\boldsymbol{\Omega}}} \, \varphi_\nu^{(\lambda)}(\widehat{\boldsymbol{\Omega}}) \right] + \lambda \langle v^l \rangle_{\nu,\lambda-1} \, \boldsymbol{a} \cdot \widehat{\boldsymbol{\Omega}} \varphi_\nu^{(\lambda)}(\widehat{\boldsymbol{\Omega}})$$

$$\left. + \langle v^l \rangle_{\nu,\lambda} (\widehat{\boldsymbol{\Omega}} \times \boldsymbol{b}) \cdot \frac{\partial}{\partial \widehat{\boldsymbol{\Omega}}} \, \varphi_\nu^{(\lambda)}(\widehat{\boldsymbol{\Omega}}) \right\}$$

$$= \sum_{\lambda=0}^{\Lambda} \left\{ \int d\widehat{\boldsymbol{\Omega}}' [\mathcal{G}_{\nu,\lambda}^{(l\uparrow)}(\widehat{\boldsymbol{\Omega}}' \cdot \widehat{\boldsymbol{\Omega}}) \, \varphi_{\nu+1}^{(\lambda)}(\widehat{\boldsymbol{\Omega}}') + \mathcal{G}_{\nu,\lambda}^{(l\downarrow)}(\widehat{\boldsymbol{\Omega}}' \cdot \widehat{\boldsymbol{\Omega}}) \, \varphi_{\nu-1}^{(\lambda)}(\widehat{\boldsymbol{\Omega}}')] - \mathcal{L}_{\nu,\lambda}^{(l\uparrow\downarrow)} \varphi_\nu^{(\lambda)}(\widehat{\boldsymbol{\Omega}}) \right\}.$$

When introducing the complementary Kronecker delta $\not\delta_{i,j} = 1 - \delta_{i,j}$, the newly appearing symbols can be written as

(105a) $$\langle v^l \rangle_{\nu,\lambda} = \int_{w_{\nu-1}}^{w_\nu} dv \, v^l (v - w_{\nu-1})^\lambda,$$

(105b) $$\mathcal{G}_{\nu,\lambda}^{(l\uparrow)} = n_1 \not\delta_{\nu,N} \int_{w_{\nu-1}}^{w_\nu} dv \, v^{l+1} (v_+ - w_\nu)^\lambda \, \sigma(v_+, \widehat{\boldsymbol{\Omega}}' \cdot \widehat{\boldsymbol{\Omega}}),$$

$$(105c) \qquad \mathcal{G}_{\nu,\lambda}^{(l\,\downarrow)} = n_2 \not{\partial}_{\nu,1} \int\limits_{w_{\nu-1}}^{w_\nu} dv\, v^{l+3}(v_- - w_{\nu-2})^\lambda (v_-)^{-2}\, \sigma(v, \widehat{\boldsymbol{\Omega}'} \cdot \widehat{\boldsymbol{\Omega}}),$$

$$(105d) \quad \mathcal{L}_{\nu,l}^{(l\,\uparrow\downarrow)} = 2\pi \int\limits_{-1}^{1} du \int\limits_{w_{\nu-1}}^{w_\nu} dv\, v^{l-1}(v - w_{\nu-1})^\lambda$$

$$\times \left\{ \not{\partial}_{\nu,1}\, n_1 v^2\, \sigma(v, u) + \not{\partial}_{\nu,N}\, n_2 (v_+)^2\, \sigma(v_+, u) \right\}.$$

In order to obtain as many equations as there are unknowns, we have to choose L, M and Λ such that they satisfy the condition

$$(106) \qquad\qquad\qquad L + M + 1 = \Lambda.$$

One physically meaningful choice would be $\Lambda = 4$, $L = 2$, $M = 1$. In this way, one recovers the exact conservation and balance laws of the kinetic model by working with smooth distribution functions.

7.2 - *Implementation*

For the numerical implementation, it is advantageous to eliminate as many unknowns as possible. Provided $L > M$, this can be achieved by expressing the continuity equations, i.e. Eq. (103), at each speed knot $\nu = 1, \ldots, N-1$ as

$$\sum_{\lambda = L+1}^{\Lambda} (w_\nu - w_{\nu-1})^\lambda\, \varphi_\nu^{(\lambda)}(\widehat{\boldsymbol{\Omega}}) = \varphi_{\nu+1}^{(0)}(\widehat{\boldsymbol{\Omega}}) - \sum_{\lambda=0}^{L} (w_\nu - w_{\nu-1})^\lambda\, \varphi_\nu^{(\lambda)}(\widehat{\boldsymbol{\Omega}}),$$

$$\vdots$$

$$\sum_{\lambda=L+1}^{\Lambda} \binom{\lambda}{m}(w_\nu - w_{\nu-1})^{\lambda-m}\, \varphi_\nu^{(\lambda)}(\widehat{\boldsymbol{\Omega}}) = \varphi_{\nu+1}^{(m)}(\widehat{\boldsymbol{\Omega}}) - \sum_{\lambda=m}^{L} \binom{\lambda}{m}(w_\nu - w_{\nu-1})^{\lambda-m}\, \varphi_\nu^{(\lambda)}(\widehat{\boldsymbol{\Omega}}),$$

$$\vdots$$

$$\sum_{\lambda=L+1}^{\Lambda} \binom{\lambda}{M}(w_\nu - w_{\nu-1})^{\lambda-M}\, \varphi_\nu^{(\lambda)}(\widehat{\boldsymbol{\Omega}}) = \varphi_{\nu+1}^{(M)}(\widehat{\boldsymbol{\Omega}}) - \sum_{\lambda=M}^{L} \binom{\lambda}{M}(w_\nu - w_{\nu-1})^{\lambda-M}\, \varphi_\nu^{(\lambda)}(\widehat{\boldsymbol{\Omega}}).$$

This can be interpreted as a set of $M + 1$ equations for the unknowns $\varphi_\nu^{(\lambda)}(\widehat{\boldsymbol{\Omega}})$ with $\lambda = L + 1, \ldots, \Lambda$. It can be solved by inversion of the $M + 1$ by $M + 1$ matrix

on the left hand side. The result can be cast in the form

$$
(107) \qquad \varphi_\nu^{(\lambda)}(\widehat{\boldsymbol{\Omega}}) = \mathfrak{M}_\nu^{(\lambda)} \cdot
\begin{pmatrix}
\varphi_\nu^{(0)}(\widehat{\boldsymbol{\Omega}}) \\
\vdots \\
\varphi_\nu^{(L)}(\widehat{\boldsymbol{\Omega}}) \\
\varphi_{\nu+1}^{(0)}(\widehat{\boldsymbol{\Omega}}) \\
\vdots \\
\varphi_{\nu+1}^{(M)}(\widehat{\boldsymbol{\Omega}})
\end{pmatrix}, \qquad
\begin{array}{l}
\lambda = L+1, \ldots, \Lambda \\
\nu = 1, \ldots, N-1
\end{array},
$$

with a $M+1$ by $L+M+2$ matrix $\mathfrak{M}_\nu$ at each interior speed knot. At the upper bound of the interval of allowed speeds, the situation is a bit different. From Eq. (102) we find a set of $M-1$ equations,

$$
\sum_{\lambda=L+3}^{\Lambda} \binom{\lambda}{m}(w_N - w_{N-1})^{\lambda-m} \varphi_N^{(\lambda)}(\widehat{\boldsymbol{\Omega}}) = -\sum_{\lambda=m}^{L+2} \binom{\lambda}{m}(w_N - w_{N-1})^{\lambda-m} \varphi_N^{(\lambda)}(\widehat{\boldsymbol{\Omega}}).
$$

By inversion of the matrix on the left hand side, we can thus express the $M-1$ unknowns $\varphi_N^{(\lambda)}(\widehat{\boldsymbol{\Omega}})$, $\lambda = L+3, \ldots, \Lambda$ in terms of $\varphi_N^{(\lambda)}(\widehat{\boldsymbol{\Omega}})$, $\lambda = m, \ldots, L+2$.

In general, the collision terms of the spline multigroup equations will still contain integrals over the solid angles $\widehat{\boldsymbol{\Omega}}$. Therefore, for a numerical implementation of these equations, the dependence of the distribution function on this variable has to be approximated appropriately. A well-established procedure is the expansion of $\varphi(v, \widehat{\boldsymbol{\Omega}})$ in terms of spherical harmonics.

8 - Non-linear spline interpolation

In this section, we present a numerical method for treating the nonlinear Boltzmann equation. In [79], a revised version of the multigroup approach to the non-linear Boltzmann equation was proposed. That method intrinsically assures the exact conservation of particles, momentum and energy and drops any *ad hoc* assumption as well as restrictions [54] imposed on the form of the shape functions. This is achieved by a kind of weighted residual method designed to fit the specific requirements of the non-linear Boltzmann equation. A shortcoming of that method, however, is the introduction of macro intervals extending over various energy groups. Furthermore, the use of rigid shape functions $\psi_i(v)$ introduces a certain degree of arbitrariness and limits the accuracy of the approach.

These restrictions can be lifted by introducing a more flexible interpolation of the distribution function $\varphi(v)$ within each energy group. This is done in an equivalent way as in the linear case. The Boltzmann equation then models the approximate distribution function in a more accurate and physically meaningful way.

We perform a polar decomposition of the velocity variable $\boldsymbol{v}$ writing $\boldsymbol{v} = v\widehat{\boldsymbol{\Omega}}$ with $v = |\boldsymbol{v}|$ and $\widehat{\boldsymbol{\Omega}} = \boldsymbol{v}/v$. Furthermore, the speed axis is subdivided into N intervals $I_\nu = [w_{\nu-1}, w_\nu)$, $\nu = 1, 2, \ldots, N-1$ located between the $N+1$ speed knots $w_0 = 0 < w_1 < \ldots < w_N$. We introduce the centers of these intervals $v_\nu = (w_\nu + w_{\nu-1})/2$ as well as their lengths $\Delta v_\nu = w_\nu - w_{\nu-1}$. All particles with speeds greater than w_N shall henceforth be neglected.

The dependence of the distribution function on the speed variable is now approximated within each energy group. In contrast to the usual multigroup approach, we do not introduce shape functions but resort to a polynomial approximation of the distribution function with respect to the speed variable v within each energy group. This ansatz reads

$$
\varphi(v\widehat{\boldsymbol{\Omega}}) \equiv v^2 f(v\widehat{\boldsymbol{\Omega}})
$$

(108)

$$
= \sum_{\nu=1}^{N} \varphi_\nu(v\widehat{\boldsymbol{\Omega}}) = \sum_{\nu=1}^{N} \chi_{I_\nu}(v) \sum_{\lambda=0}^{\Lambda} P_\nu^{(\lambda)}(v)\, \varphi_\nu^{(\lambda)}(\widehat{\boldsymbol{\Omega}}),
$$

where $\Lambda \in \mathbb{N}$ is the order of the spline approximation and $\chi_B(v)$ stands for the characteristic function of the set B. The polynomial $P_\nu^{(\lambda)}(.)$ is given by

$$
(109) \qquad\qquad P_\nu^{(\lambda)}(v) = \sqrt{\frac{2}{\Delta v_\nu}}\, P^{(\lambda)}\!\left(\frac{2(v - v_\nu)}{\Delta v_\nu}\right).
$$

Here, $P^{(\lambda)}(.)$ denotes the Legendre polynomial of degree λ and consequently we can say that the distribution function is approximated by a polynomial of degree Λ within each energy group I_ν. The new unknowns of this approach are the $N \times (\Lambda + 1)$ functions $\varphi_\nu^{(\lambda)}(\widehat{\boldsymbol{\Omega}})$ that, of course, also depend on $\boldsymbol{x}$ and on t.

At the borders of the energy groups, we demand the continuity of the distribution function $\varphi(v\widehat{\boldsymbol{\Omega}})$ and of some of its derivatives with respect to v, say up to the M-th order. This yields a set of $(M+1) \times (N-1)$ equations,

$$
(110a) \qquad \varphi_\nu(w_\nu\widehat{\boldsymbol{\Omega}}) = \varphi_{\nu+1}(w_\nu\widehat{\boldsymbol{\Omega}}) \qquad\qquad \nu = 1, \ldots, N-1,
$$

$$
(110b) \qquad \varphi_\nu'(w_\nu\widehat{\boldsymbol{\Omega}}) = \varphi_{\nu+1}'(w_\nu\widehat{\boldsymbol{\Omega}}) \qquad\qquad \nu = 1, \ldots, N-1,
$$

$$
\vdots \qquad\qquad\qquad \vdots
$$

$$
(110c) \qquad \varphi_\nu^{(M)}(w_\nu\widehat{\boldsymbol{\Omega}}) = \varphi_{\nu+1}^{(M)}(w_\nu\widehat{\boldsymbol{\Omega}}) \qquad\qquad \nu = 1, \ldots, N-1,
$$

where the prime denotes the first and (M) denotes the M-th derivative with respect to v. This is a set of $(M + 1) \times (N - 1)$ equations. Consequently, to retain some degrees of freedom for the function φ, M has to be chosen smaller than Λ, $M < \Lambda$. Furthermore, from the definition of φ, we have the boundary conditions at the origin,

$$(111) \qquad \varphi(0\widehat{\boldsymbol{\Omega}}) = \varphi'(0\widehat{\boldsymbol{\Omega}}) = 0 \,.$$

If $M > 1$ it seems natural to put the higher derivatives to zero at $v = w_N$. We obtain a set of $(M + 1) \times N$ equations from continuity relations if we demand

$$(112) \qquad \varphi''(w_N \widehat{\boldsymbol{\Omega}}) = \varphi'''(w_N \widehat{\boldsymbol{\Omega}}) = \ldots = \varphi^{(M)}(w_N \widehat{\boldsymbol{\Omega}}) = 0 \,.$$

To derive the spline-multigroup equations, we insert the ansatz, i.e. Eq. (108), into the nonlinear Boltzmann equation

$$(113) \qquad \frac{\partial \varphi(v\widehat{\boldsymbol{\Omega}})}{\partial t} + v\,\widehat{\boldsymbol{\Omega}} \cdot \frac{\partial \varphi(v\widehat{\boldsymbol{\Omega}})}{\partial \boldsymbol{x}} = J[\varphi, \varphi],$$

where, as usual, $J[\varphi, \varphi]$ stands for the nonlinear collision term expressed in the scattering kernel formulation,

$$
\begin{aligned}
J[\varphi, \varphi] = \int_0^\infty dv' \int_0^\infty dv'' \int d\widehat{\boldsymbol{\Omega}}' \int d\widehat{\boldsymbol{\Omega}}'' \, g(|v'\,\widehat{\boldsymbol{\Omega}}' - v''\,\widehat{\boldsymbol{\Omega}}''|)\, \Pi(v'\,\widehat{\boldsymbol{\Omega}}', v''\,\widehat{\boldsymbol{\Omega}}'' \to v\widehat{\boldsymbol{\Omega}}) \\
\times \varphi(v', \widehat{\boldsymbol{\Omega}})\, \varphi(v'', \widehat{\boldsymbol{\Omega}}'') - \varphi(v, \widehat{\boldsymbol{\Omega}}) \int_0^\infty dv' \int d\widehat{\boldsymbol{\Omega}}' \, g(|v\widehat{\boldsymbol{\Omega}} - v'\,\boldsymbol{\Omega}'|)\, \varphi(v', \widehat{\boldsymbol{\Omega}}) \,.
\end{aligned}
$$

(114)

This formulation of the scattering term is best suited for proving the conservation of mass, momentum and kinetic energy of the gas. The symbol g stands for the microscopic collision frequency $g(V) = V\sigma_0(V)$, where σ_0 is the total cross section depending on the relative speed V of the colliding particles. In the case of isotropic scattering, the kernel Π corresponding to the Boltzmann equation is given by

$$(115) \quad \Pi(v'\,\widehat{\boldsymbol{\Omega}}', v''\,\widehat{\boldsymbol{\Omega}}'' \to v\widehat{\boldsymbol{\Omega}}) = \frac{1}{\pi}\, \frac{v^2}{|v'\,\widehat{\boldsymbol{\Omega}}' - v''\,\widehat{\boldsymbol{\Omega}}''|}\, \delta((v\widehat{\boldsymbol{\Omega}} - v'\,\widehat{\boldsymbol{\Omega}}') \cdot (v\widehat{\boldsymbol{\Omega}} - v''\,\widehat{\boldsymbol{\Omega}}'')) \,.$$

Because of the Dirac delta function, the gain term in Eq. (114) actually collapses to the familiar fivefold integral. Since the speeds of the gas particles are restricted to the interval $[0, w_N)$, we put $\Pi = 0$ whenever $v > w_N$ or $v_*^2 = v'^2 + v''^2 - v^2 > w_N^2$.

Then we multiply the Boltzmann equation by $P_v^{(l)}(v)$, where $l = 0, 1, 2, \ldots, L$,

$\nu = 1, 2, \ldots, N$ and integrate over the energy group $I_\nu = [w_{\nu-1}, w_\nu)$. This yields a set of $(L + 1) \times N$ multigroup equations. In order to reproduce the important conservation laws concerning particle density, momentum density and kinetic energy density,

$$(116a) \qquad \int_0^\infty dv \int d\widehat{\boldsymbol{\Omega}}\, \Pi(v'\,\widehat{\boldsymbol{\Omega}}', v''\widehat{\boldsymbol{\Omega}}'' \to v\widehat{\boldsymbol{\Omega}}) = 1\,,$$

$$(116b) \qquad \int_0^\infty dv \int d\widehat{\boldsymbol{\Omega}}\, v\,\widehat{\boldsymbol{\Omega}}\, \Pi(v'\,\widehat{\boldsymbol{\Omega}}', v''\widehat{\boldsymbol{\Omega}}'' \to v\widehat{\boldsymbol{\Omega}}) = \frac{1}{2}\,(v'\,\widehat{\boldsymbol{\Omega}}' + v''\widehat{\boldsymbol{\Omega}}'')\,,$$

$$(116c) \qquad \int_0^\infty dv \int d\widehat{\boldsymbol{\Omega}}\, v^2\, \Pi(v'\,\widehat{\boldsymbol{\Omega}}', v''\widehat{\boldsymbol{\Omega}}'' \to v\widehat{\boldsymbol{\Omega}}) = \frac{1}{2}\,(v'^2 + v''^2)\,,$$

we will need at least $L = 2$. Of course, choices $L > 2$ are also permissible. As already stated in [**79**], with $L = 3$ it is possible to reproduce the left hand side of the third order moment equation that gives rise to the constitutive equation for heat flow.

The correct relation between the order of the spline interpolation Λ, the order of continuity M and the maximal power L of v is given by

$$(117) \qquad \Lambda = M + L + 1\,.$$

In order to state the resulting multigroup equations in a compact form, we introduce the following integrals:

$$(118a) \qquad \langle v^k \rangle_\nu^{(l)(\lambda)} = \int_{w_{\nu-1}}^{w_\nu} dv\, v^k P_\nu^{(l)}(v)\, P_\nu^{(\lambda)}(v)\,,$$

$$(118b) \qquad g_{\nu,\nu_*}^{(l)(\lambda)(\lambda_*)}(\widehat{\boldsymbol{\Omega}}\cdot\widehat{\boldsymbol{\Omega}}_*) = \int_{w_{\nu-1}}^{w_\nu} dv\, P_\nu^{(l)}(v)\, P_\nu^{(\lambda)}(v) \int_{w_{\nu_*-1}}^{w_{\nu_*}} dv_*\, P_{\nu_*}^{(\lambda_*)}(v_*)\, g(|v\widehat{\boldsymbol{\Omega}} - v_*\widehat{\boldsymbol{\Omega}}_*|)\,,$$

$$(118c) \qquad \begin{aligned} g_{\nu',\nu''}^{(l)(\lambda')(\lambda'')}(\widehat{\boldsymbol{\Omega}}'\cdot\widehat{\boldsymbol{\Omega}}'')\, \Pi_{\nu',\nu'';\nu}^{(l)(\lambda')(\lambda'')}(\widehat{\boldsymbol{\Omega}}', \widehat{\boldsymbol{\Omega}''} \to \widehat{\boldsymbol{\Omega}}) &= \int_{w_{\nu-1}}^{w_\nu} dv\, P_\nu^{(l)}(v) \int_{w_{\nu'-1}}^{w_{\nu'}} dv' \int_{w_{\nu''-1}}^{w_{\nu''}} dv'' \\ &\times P_{\nu'}^{(\lambda')}(v')\, P_{\nu''}^{(\lambda'')}(v'')\, g(|v'\,\widehat{\boldsymbol{\Omega}}' - v''\widehat{\boldsymbol{\Omega}}''|)\, \Pi(v'\,\widehat{\boldsymbol{\Omega}}', v''\widehat{\boldsymbol{\Omega}}'' \to v\widehat{\boldsymbol{\Omega}})\,. \end{aligned}$$

Equation (118a) is an average over the energy group ν of the k-th power of the speed v. As a consequence of the orthogonality of the Legendre polynomials, we

obtain for the case $k = 0$

$$(119) \qquad \langle 1 \rangle_\nu^{(l)(\lambda)} = \int_{w_{\nu-1}}^{w_\nu} dv \, P_\nu^{(l)}(v) \, P_\nu^{(\lambda)}(v) = \frac{2}{2l+1} \, \delta_{l,\lambda}.$$

Equations (118b) and (118c) are the integrated versions of the collision frequency g and the scattering kernel Π, respectively.

By using these definitions and exchanging the orders of sums and integrals, we obtain the following set of *non-linear Legendre-multigroup* equations

$$
\frac{2}{2l+1} \frac{\partial \varphi_\nu^{(l)}(\widehat{\boldsymbol{\Omega}})}{\partial t} + \sum_{\lambda=0}^{\Lambda} \langle v \rangle_\nu^{(l)(\lambda)} \widehat{\boldsymbol{\Omega}} \cdot \frac{\partial \varphi_\nu^{(\lambda)}(\widehat{\boldsymbol{\Omega}})}{\partial \boldsymbol{x}}
$$

$$
(120) = \sum_{\lambda',\lambda''=0}^{\Lambda} \sum_{\nu',\nu''=1}^{N} \int d\widehat{\boldsymbol{\Omega}}' \int d\widehat{\boldsymbol{\Omega}}'' \, g_{\nu',\nu''}^{(l)(\lambda')(\lambda'')}(\widehat{\boldsymbol{\Omega}}' \cdot \widehat{\boldsymbol{\Omega}}'') \Pi_{\nu',\nu'';\nu}^{(l)(\lambda')(\lambda'')}(\widehat{\boldsymbol{\Omega}}', \widehat{\boldsymbol{\Omega}}'' \to \widehat{\boldsymbol{\Omega}}) \varphi_{\nu'}^{(\lambda')}(\widehat{\boldsymbol{\Omega}}') \varphi_{\nu''}^{(\lambda'')}(\widehat{\boldsymbol{\Omega}}'')
$$

$$
- \sum_{\lambda,\lambda_*=0}^{\Lambda} \varphi_\nu^{(\lambda)}(\widehat{\boldsymbol{\Omega}}) \sum_{\nu_*=1}^{N} \int d\widehat{\boldsymbol{\Omega}}_* \, \varphi_{\nu_*}^{(\lambda_*)}(\widehat{\boldsymbol{\Omega}}_*) \, g_{\nu,\nu_*}^{(l)(\lambda)(\lambda_*)}(\widehat{\boldsymbol{\Omega}} \cdot \widehat{\boldsymbol{\Omega}}_*)
$$

approximating the continuous Boltzmann equation (113).

Remark. The advantage of working with Legendre polynomials lies in the fact that the sum in front of the temporal derivative collapses to one single term. When respecting the matching condition (117), the spline multigroup equations (120) combined with the continuity relations (110)-(112) represent a closed set of $(\Lambda+1) \times N$ integro-differential equations for the $(\Lambda+1) \times N$ unknowns $\varphi_\nu^{(\lambda)}$. ∎

Following the lines of [79], it can be shown that the spline-multigroup approximation displays particle, momentum and kinetic energy conservation provided $\Lambda \geqslant 2$ and $L \geqslant 2$.

9 - Conclusion

This paper reviews different procedures of kinetic energy discretization in the extended kinetic theory and their applications. Boltzmann transport equations are solved numerically within the approximations of a semi-continuous formulation or a multigroup approach.

Semi-continuous Boltzmann equations are found to be well suited for treating problems, where external force terms can be neglected. These models are obtained through a partition of the positive real axes of kinetic energies into a number

of energy groups. Within each group, the distribution function is approximated by a constant value.

Semi-continuous models display excellent properties. The relaxation behavior of such models agrees to a high extent with the exact solution of the BKW mode for Maxwell molecules. In fact, for a sufficient number of groups, the discrepancy is found to be less than 0.2%. It can be expected that semi-continuous models reflect the correct relaxation behavior also for general interaction models.

An extension of the discretization concept to a mixture of elastically and inelastically scattering gas particles interacting with monochromatic photons is formulated. The resulting model reflects all major aspects (conservation laws, equilibria, Planck's law of radiation and H-functional) of the continuous kinetic description. The impact of an intense laser pulse that is in resonance with the transition of a two-level atom is studied numerically. In case of Maxwell molecules, far-from-equilibrium distribution functions are observed during the relaxation process. Moreover, the extended semi-continuous kinetic model is applied to the simulation of thermal acoustic experiments. To this end, it is solved by applying a P_3 approximation in one-dimensional spatial geometry.

Different masses of the involved gas particles are considered to be the major obstacle in the formulation of discrete velocity models for a mixture of chemically reacting gases. Due to the greater flexibility of semi-continuous models, i.e. the continuous solid angles in velocity space, the difficulty can be overcome in a semi-continuous formulation. This is achieved for arbitrary mass ratios by adapting the ranges of integration over the solid angles properly. The resulting semi-continuous model governs the evolution of a four component gas mixture undergoing bimolecular chemical reactions. The major advantage as compared to scalar Boltzmann equations is the capability of treating spatially dependent phenomena. As a first step, however, space homogeneous problems are solved, and the evolution of the distribution function is studied. During fast exothermic reactions, especially the reactants exhibit highly athermal kinetic energy distributions. When a threshold is also accounted for in the exothermic reaction, delayed ignition of the reaction can be observed.

The overlapping multigroup approach is a first attempt to tackle consistently kinetic problems involving an external force term within the framework of multigroup approaches. Based on the method of weighted residuals, this scheme takes into account electric and magnetic forces acting on charged particles without any additional assumptions. It is applied to the study of an extended Lorentz gas model. To this end, a P_1 approximation is carried out and solved numerically. Problems related to the use of rigid shape functions are expected to be overcome by resorting to a spline interpolation of the speed variable.

Due to the importance of all three conservation laws in nonlinear kinetic theory, the concept of multigroup schemes has to be generalized if one wants to apply it to nonlinear Boltzmann equations. One single weight function is not enough to satisfy the conservation of mass, momentum and kinetic energy. A fully conservative scheme is achieved by introducing at least three weight functions and by extending the speed-integration over so-called macro intervals. The scheme can be made more flexible and numerically stable when working with orthogonal polynomials within each energy group.

References

[1]   C. CERCIGNANI, *The Boltzmann equation and its applications*, Springer, New York 1988.

[2]   C. CERCIGNANI, R. ILLNER and M. PULVIRENTI, *The mathematical theory of dilute gases*, Springer, New York 1994.

[3]   J. C. LIGHT, J. ROSS and K. E. SHULER, *Rate coefficients, reaction cross sections and microscopic reversibility*, in *kinetic processes in gases and plasmas*, ed. A. R. Hochstim, Academic Press, New York 1969, 281-320.

[4]   M. KROOK and T. T. WU, *Exact solutions of the Boltzmann equation*, Phys. Fluids **20** (1977), 1589-1595.

[5]   M. KROOK and T. T. WU, *Exact solutions of Boltzmann equations for multicomponent systems*, Phys. Rev. Lett. **38** (1977), 991-993.

[6]   M. H. ERNST, *Nonlinear model-Boltzmann equations and exact solutions*, Phys. Rep. **78** (1981), 1-171.

[7]   M. H. ERNST, *Exact solutions of the nonlinear Boltzmann equation*, J. Statist. Phys. **34** (1984), 1001-1017.

[8]   F. SCHÜRRER and M. SCHALER, *Exact solutions of the Boltzmann equation in the VHP model with removal interaction*, J. Statist. Phys. **66** (1992), 1045-1058.

[9]   D. RUPP, G. DUKEK and T. F. NONNENMACHER, *Particle transport in a host medium with an external source: exact solutions for a nonlinear homogeneous Boltzmann equation*, Z. Angew. Math. Phys. **39** (1988), 605-618.

[10]   H. CORNILLE, *Oscillating and absolute Maxwellians: exact solutions for $(d > 1)$ dimensional Boltzmann equations*, J. Math. Phys. **27** (1986), 1373-1386.

[11]   V. C. BOFFI and M. TORRISI, *Methods of similarity analysis in the study of nonlinear dynamics of a gas mixture*, Transport Theory Statist. Phys. **19** (1990), 139-159.

[12]   G. SPIGA, *Rigorous solution to the extended kinetic equations for homogeneous gas mixtures*, in Lecture Notes in Mathematics, vol. 1460, ed. G. Toscani, V. Boffi and S. Rionero, Springer, New York 1990.

[13] H. CABANNES and DANG-HONG-TIEM, *Exact solutions for a semi-continuous model of the Boltzmann equation*, C. R. Acad. Sci. Paris **318** (1994), 1583-1590.

[14] G. KÜGERL and F. SCHÜRRER, *Energy conservation and H-theorem in the scalar nonlinear Boltzmann equation and its multigroup representation*, Phys. Lett. A **148** (1990), 158-163.

[15] G. KÜGERL and F. SCHÜRRER, *Scalar nonlinear Boltzmann equation for gas-mixtures*, Z. Angew. Math. Phys. **42** (1991), 363-369.

[16] G. KÜGERL and F. SCHÜRRER, *On the relaxation of binary hard-sphere gases*, Physica A **190** (1992), 186-202.

[17] G. A. BIRD, *Molecular gas dynamics and the direct simulation of gas flows*, Oxford University Press, Oxford 1994.

[18] U. FRISCH, B. HASSLACHER and Y. POMEAU, *Lattice gas automata for Navier Stokes equations*, Phys. Rev. Lett. **56** (1986), 1505-1508.

[19] R. GATIGNOL, *Théorie cinétique des gaz à répartition discrète des vitesses*, Lecture notes in Physics, vol. 36, Springer, Berlin, New York 1975.

[20] H. CABANNES, *The discrete model of the Boltzmann equation*, Transport Theory Statist. Phys. **16** (1987), 809-836.

[21] R. ILLNER and T. PLATKOWSKI, *Discrete velocity models of the Boltzmann equation: A survey on the mathematical aspects of the theory*, SIAM Rev. **30** (1988), 213-255.

[22] R. MONACO and L. PREZIOSI, *Fluid dynamic application of the discrete Boltzmann equation*, World Scientific, Singapore 1991.

[23] N. BELLOMO and T. GUSTAFSSON, *The discrete Boltzmann equation: a review of the mathematical aspects of the initial and boundary value problem*, Rev. Math. Phys. **3** (1991), 137-162.

[24] P. REITERER, C. REITSHAMMER, F. SCHÜRRER, F. HANSER and T. EITZENBERGER, *New discrete model Boltzmann equations for arbitrary partitions of the velocity space*, J. Statist. Phys. **98** (2000), 419-440.

[25] M. H. ERNST, *Temperature and heat conductivity in cellular automata fluids*, in Discrete models of fluid-dynamics, ed. A. Alves, World Scientific, Singapore 1991.

[26] C. CERCIGNANI, *On the thermodynamics of a discrete velocity gas*, Transport Theory Statist. Phys. **23** (1994), 1-8.

[27] F. SCHÜRRER, P. GRIEHSNIG and G. KÜGERL, *The nonlinear Boltzmann equation including internal degrees of freedom*, Phys. Fluids A **4** (1992), 2739-2746.

[28] P. GRIEHSNIG, F. SCHÜRRER and G. KÜGERL, *Kinetic theory for particles with internal degrees of freedom*, in Rarefied gas dynamics: theory and simulations, ed. B. D. Shizgal and D. P. Weaver, vol. 159, Progress in Astronautics and Aeronautics, AIAA, Washington DC 1994, 581-9.

[29] C. R. GARIBOTTI and G. SPIGA, *Boltzmann equation for inelastic scattering*, J. Phys. A **27** (1994), 2709-2717.

[30] S. I. PAI, *Radiation gas dynamics*, Springer, Wien 1966.

[31]   A. ROSSANI, G. SPIGA and R. MONACO, *Kinetic approach for two-level atoms interacting with monochromatic photons*, Mech. Res. Comm. **24** (1997), 237-242.

[32]   A. ROSSANI and G. SPIGA, *Kinetic theory with inelastic interactions*, Transport Theory Statist. Phys. **27** (1998), 273-287.

[33]   A. MAJORANA, *Space homogeneous solutions of the Boltzmann equation describing electron-phonon interactions in semiconductors*, Transport Theory. Statist. Phys. **20** (1991), 261-279.

[34]   A. MAJORANA, *Conservation laws from the Boltzmann equation describing electron-phonon interactions in semiconductors*, Transport Theory Statist. Phys. **22** (1993), 849-859.

[35]   I. PRIGOGINE and E. XHROUET, *On the perturbation of Maxwell distribution function by chemical reactions in a gas*, Physica **15** (1949), 913-932.

[36]   I. PRIGOGINE and M. MAHIEU, *Sur la perturbation de la distribution de Maxwell par des réactions chimiques en phase gazeuse*, Physica **16** (1950), 51-64.

[37]   V. C. BOFFI and A. ROSSANI, *On the Boltzmann system of a mixture of reacting gases*, Z. Angew Math. Phys. **41** (1990), 254-268.

[38]   G. KÜGERL, *A consistent numerical method for the solution of the Boltzmann equation for inelastic and reactive scattering*, Z. Angew. Math. Phys. **42** (1991), 821-836.

[39]   G. KÜGERL, *Solution of the Boltzmann equation for a reacting gas mixture*, Phil. Trans. R. Soc. Lond. A **342** (1993), 413-438.

[40]   A. ROSSANI and G. SPIGA, *A note on the kinetic theory of chemically reacting gases*, Phys. A **272** (1999), 563-573.

[41]   G. SPIGA, *On extended kinetic theory with chemical reaction*, in Nonlinear kinetic theory and mathematical aspects of hyperbolic systems, ed. V. C. Boffi, F. Bampi and G. Toscani, vol. 9, Ser. Adv. Math. App. Sci., World Scientific, Singapore (1993), 242-252.

[42]   M. GROPPI and G. SPIGA, *Kinetic approach to chemical reactions and inelastic transitions in a rarefied gas*, J. Math. Chem. **26** (1999), 197-219.

[43]   A. ROSSANI, *Fokker Planck approximation of the linear Boltzmann equation with inelastic scattering: study of the distribution function for chareged particles subjected to an external electric field*, Riv. Mat. Univ. Parma **6** (1997), 35-45.

[44]   M. FONTANA and G. SPIGA, *Application of extended kinetic theory to particle transport with inelastic scattering*, Z. Angew Math. Phys. **47** (1996), 539-552.

[45]   J. BANASIAK, G. FROSALI and G. SPIGA, *Asymptotic analysis for a particle transport equation with inelastic scattering in extended kinetic theory*, Math. Models Methods. Appl. Sci. **8** (1998), 851-874.

[46]   P. EHERENFEST and T. EHRENFEST, *Begriffliche Grundlagen der statistischen Auffassung in der Mechanik*, in Encyklop. d. math. Wissenschaften IV, vol. 2, 1912.

[47]   A. V. BOBYLEV and G. SPIGA, *On a model transport equation with inelastic scattering*, SIAM J. Appl. Math. **58** (1998), 1128-1137.

[48] G. L. CARAFFINI, B. D. GANAPOL and G. SPIGA, *A multigroup approach to the non-linear extended Boltzmann equation*, Il Nuovo Cimento D **17** (1995), 129-142.

[49] C. CERCIGNANI, C. SGARRA and M. LAMPIS, *On the relation between the scattering kernel and the standard formulation of the Boltzann equation*, Il Nuouvo Cimento B **101** (1988), 523-531.

[50] V. C. BOFFI, V. PROTOPOPESCU and G. SPIGA, *On the Equivalence between the probabilistic, kinetic and scattering kernel formulation of the Boltzmann equation*, Physica A **164** (1990), 400-410.

[51] N. BELLOMO and E. LONGO, *A new discretized model in nonlinear kinetic theory: the semicontinuous Boltzmann equation*, Math. Models Methods Appl. Sci. **1** (1991), 113-123.

[52] E. LONGO, L. PREZIOSI and N. BELLOMO, *The semicontinuous Boltzmann equation: towards a model for fluiddynamic applications*, Math. Models Methods Appl. Sci. **3** (1993), 65-93.

[53] L. PREZIOSI and E. LONGO, *On a conservative polar discretization of the Boltzmann equation*, Japan J. Indust. Appl. Math. **14** (1997), 399-435.

[54] G. SPIGA, *A Note on speed discretization in kinetic theory via the scattering kernel formulation of the Boltzmann equation*, Transport Theory Statist. Phys. **26** (1997), 243-251.

[55] A. ROSSANI and G. SPIGA, *Extended thermodynamics of a two group model of the Boltzmann equation*, Transport Theory Statist. Phys. **25** (1996), 699-712.

[56] H. GRAD, *On the kinetic theory of rarefied gases*, Comm. Pure Appl. Math. **2** (1949), 331-407.

[57] H. GRAD, *Principles of the kinetic theory of gases*, in Handbuch der Physik, vol. XII, ed. S. Flügge, Springer, Berlin (1958), 205-294.

[58] M. MÜLLER and T. RUGGERI, *Extended thermodynamics*, Springer, Berlin 1993.

[59] R. CAVAZZONI and G. SPIGA, *A note on Grad's 13 moment expansion in extended kinetic theory*, Riv. Mat. Univ. Parma **4** (1995), 263-272.

[60] W. KOLLER, *P_1 Approximation of the nonlinear semi-continuous Boltzmann equation*, Riv. Mat. Univ. Parma **2** (1999), 159-181.

[61] W. KOLLER and F. SCHÜRRER, *P_N Approximation of the nonlinear semi-continuous Boltzmann equation*, Transport Theory Statist Phys. (in print).

[62] E. B. CUMMINGS, *Laser-induced thermal acoustics*, PhD thesis, California Institute of Technology, Pasadena CA 91125, 1995.

[63] J. OXENIUS, *Kinetic theory of particles and photons*, Springer, Berlin 1986.

[64] W. KOLLER, F. HANSER and F. SCHÜRRER, *A semi-continuous extended kinetic model*, J. Phys. A **33** (2000), 3417-3430.

[65] M. M. R. WILLIAMS, *Mathematical methods in particle transport theory*, Butterworth & Co, London 1971.

[66] G. JAFFÉ, *Zur Methodik der kinetischen Gastheorie*, Japan J. Indust. Appl. Math. **6** (1930), 195-252.

[67] V. C. BOFFI and G. SPIGA, *Continuity equation in the study of nonlinear particle-transport evolution problems*, Phys. Rev. A **29** (1984), 782-790.

[68] F. SCHÜRRER, *Die Kugelfunktionsmethode als Lösungsansatz für die nichtlineare Boltzmann-Gleichung*, Atomkernenergie-Kerntechnik **6** (1985), 238-242.

[69] G. KÜGERL and F. SCHÜRRER, P^{KLM} *Expansion of the scattering kernel of the nonlinear Boltzmann equation and its convergence rate*, Phys. Rev. A **39** (1989), 1429-1440.

[70] G. KÜGERL and F. SCHÜRRER, *The P_N method in the kinetic theory of gases*, Z. Naturforsch. **47a** (1992), 925-934.

[71] N. BELLOMO, *Lecture notes on the mathematical theory of the Boltzmann equation*, World Scientific, Singapore 1995.

[72] R. N. SILVER, H. RÖDER, A. F. VOTER and J. D. KRESS, *Kernel polynomial approximations for densities of states and spectral functions*, Journal Comp. Phys. **124** (1996), 115-130.

[73] P. H. PAUL, R. L. FARROW and P. M. DANEHY, *Gas-phase thermal-grating contributions to four-wave mixing*, J. Opt. Soc. Am. B **12** (1995), 384-392.

[74] W. KOLLER, *A semi-continuous extended kinetic model for bimolecular chemical reactions*, J. Phys. A **33** (2000), 6081-6094.

[75] L. LAPIDUS and G. F. PINDER, *Numerical solutions of partial differential equations in science and engineering*, John Wiley and Sons, New York 1982.

[76] A. F. HENRY, *Nuclear reactor analysis*, MIT press, Cambridge 1975.

[77] W. KOLLER, A. ROSSANI, F. SCHÜRRER and G. SPIGA, *Overlapping multigroup approach to a linear extended Boltzmann equation*, J. Appl. Math. Phys. **52** (2001), 231-253.

[78] A. ROSSANI and A. M. SCARFONE, *Tsallis distribution functions for charged particles in electric and magnetic fields*, Physica A. **282** (2000), 212-224.

[79] W. KOLLER, A. ROSSANI, F. SCHÜRRER and G. SPIGA, *A conservative multigroup approach to the nonlinear Boltzmann equation*, Mech. Res. Com. (in print).

Abstract

We review current strategies of energy discretization of the Boltzmann equation in the framework of extended kinetic theory. When external fields can be neglected, the semi-continuous Boltzmann equation yields a sound basis for various applications. A three component gas mixture interacting with monochromatic photons as well as a four component gas mixture undergoing chemical reactions are dealt with by means of this approach. The model equations reflect all major aspects of a continuous kinetic description, such as, conservation laws, equilibria and an H-theorem. Spatially dependent problems are treated by applying an expansion of the distribution function in terms of Legendre polynomials with respect to the polar angle. The resulting PDE in real space and time are solved by an implicit finite differencing scheme combined with an operator splitting method. In the presence of external fields, an overlapping multigroup method (with a spline-interpolation method as its extension) is developed for numerical studies. Furthermore, a formulation of a multigroup approach consistent with the non-linear Boltzmann equation is presented.

* * *